Conformational Gating of Charge Separation in Porphyrin Oligomer-Fullerene Systems

Supporting Information

Mélina Gilbert, ¤ *Louisa J. Esdaile,* † *Marie Hutin,* † *Katsutoshi Sawada,* † *Harry L. Anderson,* † *and Bo Albinsson* ¤

¤ Department of Chemical and Biological Engineering / Physical Chemistry

Chalmers University of Technology, 412 96 Göteborg, Sweden

Email: balb@chalmers.se

† Department of Chemistry, Oxford University,

Chemistry Research Laboratory 12 Mansfield Road, Oxford OX1 3TA, UK

Email: harry.anderson@chem.ox.ac.uk

Table of Contents

Titration of P_4 and P_4C_{60} with the octadentate template T8

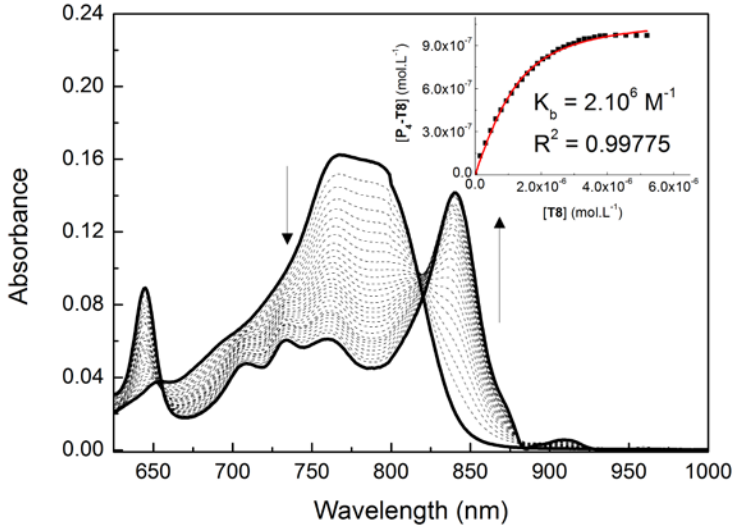

Figure S1. The Q band region of $\mathbf{P_4}$. A solution of $\mathbf{P_4}$ titrated by the octadentate ligand **T8** in DCM/Toluene (60/40) with 0.1% pyridine added. The total concentration of $\mathbf{P_4}$ was approximately 0.94 µM. A weak baseline distortion at 910 nm is observed and is attributed due to the experimental conditions. The baseline was initially measured in DCM with 0.1% pyridine added. For solubility reason, the ligand **T8** was dissolved in Toluene, and thus during the titration consecutive additions of **T8** give rise to a slight baseline distortion at 910 nm. Inset concentration of $\mathbf{P_4}$-**T8** complex formed vs. concentration of template **T8** added with fitted binding curve yielding K_b= 2 x 10^6 M^{-1}.

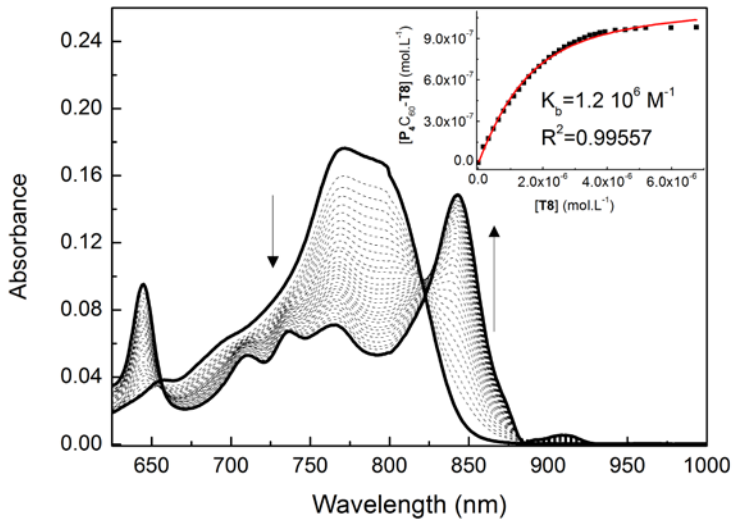

Figure S2. The Q band region of $\mathbf{P_4}C_{60}$. A solution of $\mathbf{P_4}C_{60}$ titrated by the octadentate ligand **T8** in DCM/Toluene (60/40) with 0.1% pyridine added. The total concentration of $\mathbf{P_4}C_{60}$ was approximately 1 µM. A weak baseline distortion is observed at 910 nm and is attributed to the experimental conditions as explained previously. Inset concentration of $\mathbf{P_4}C_{60}$-**T8** complex formed vs. concentration of template **T8** added with fitted binding curve yielding K_b= 1.2 x 10^6 M^{-1}.

Titration of P_6C_{60} with the octadentate template T8

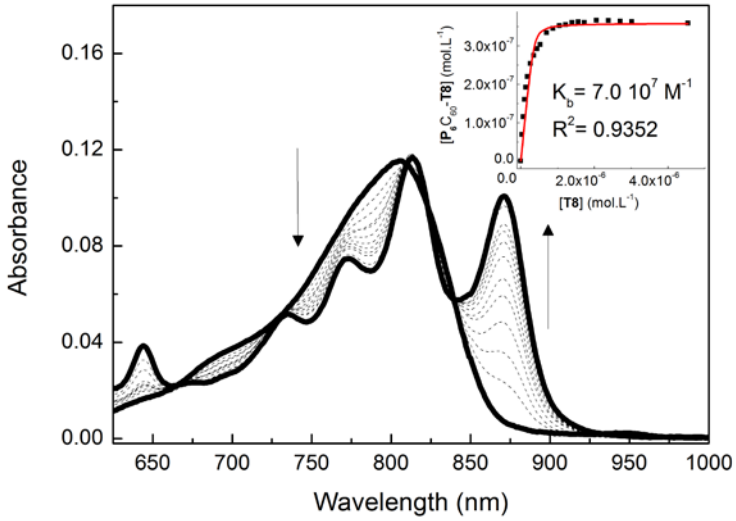

Figure S3. The Q band region of $\mathbf{P_6C_{60}}$. A solution of $\mathbf{P_6C_{60}}$ titrated by the octadentate ligand **T8** in DCM/Toluene (60/40) with 0.1% pyridine added. The total concentration of $\mathbf{P_6C_{60}}$ was approximately 0.40 µM. Inset concentration of $\mathbf{P_6C_{60}}$**-T8** complex formed vs. concentration of template **T8** added with fitted binding curve yielding K_b= 7.0 x 10^7 M^{-1}.

Emission Spectra of P_6 and P_6C_{60} at 300 K

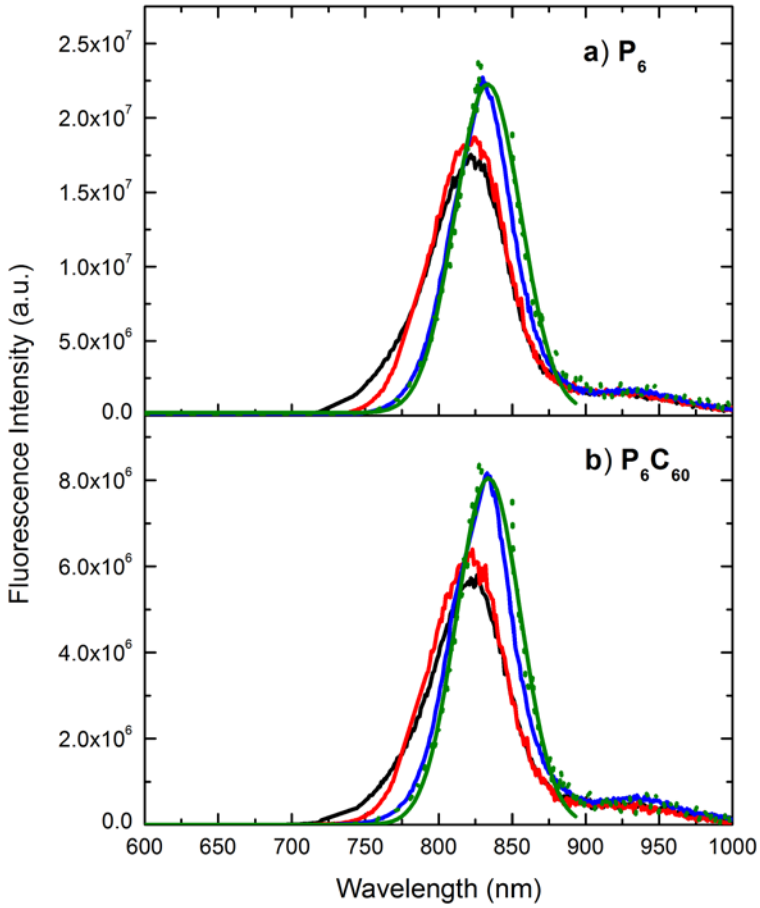

Figure S4. Fluorescence spectra of (a) $\mathbf{P_6}$ and (b) $\mathbf{P_6}C_{60}$ excited at 730 nm (black), 780 nm (red), 820 nm (blue) and 840 nm (green) in 2-MTHF with 1% pyridine added at 300 K. All emission spectra were corrected in order to get equal absorbance at all excitation wavelengths and facilitate the comparison. For all excitation wavelengths, emission spectra were measured in two steps by recording the emission below and above the excitation wavelength with a gap of ~20 nm centered on the excitation wavelength to avoid scattering of the excitation light. For the excitation wavelength 840 nm, this unfortunately led to a gap in the raw data in the region of the emission peak. Therefore the raw data for λ_{exc} = 840 nm are presented in dotted lines and are fitted with a Gaussian function (solid lines) to help the reader to visualize the whole emission peak.

Emission Spectra of P_6 and P_6C_{60} at 180 K

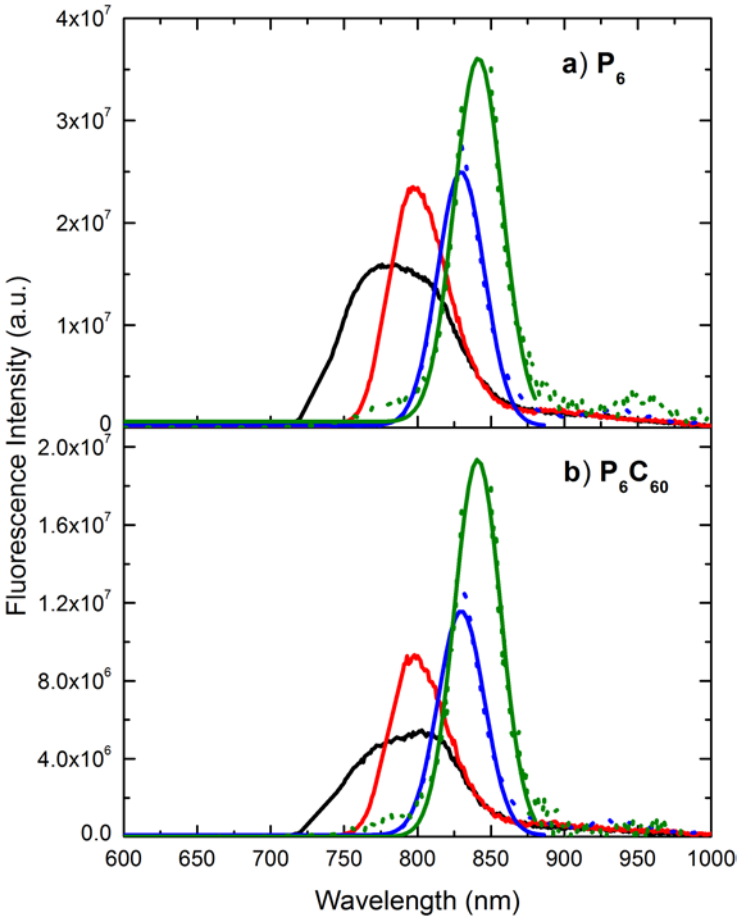

Figure S5. Fluorescence spectra of (a) $\mathbf{P_6}$ and (b) $\mathbf{P_6}C_{60}$ excited at 730 nm (black), 780 nm (red), 820 nm (blue) and 840 nm (green) in 2-MTHF with 1% pyridine added at 180 K. All emission spectra were corrected in order to get equal absorbance at all excitation wavelengths and facilitate the comparison. As mentioned previously, emission spectra were measured in two steps by recording the emission below and above the excitation wavelength with a gap of ~20 nm centered on the excitation wavelength to avoid scattering of the excitation light. Due to this gap, the raw data for λ_{exc} = 820 nm and λ_{exc} = 840 nm are presented in dotted lines and are fitted with a Gaussian function (solid lines) to help the reader to visualize the whole emission peak.

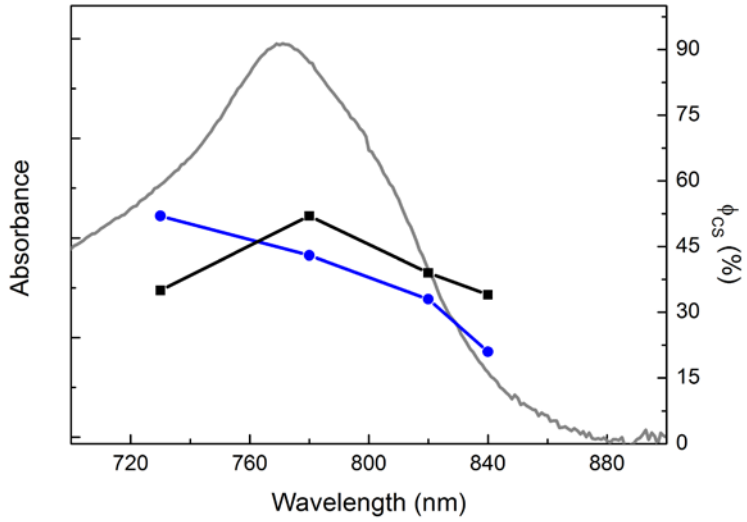

Figure S6. Quantum yield for charge separation as function of the excitation wavelength for $\mathbf{P_6}C_{60}$ in 2-MTHF with 1% pyridine added at 180 K based on steady-state (blue) and time-resolved fluorescence (black) measurements. The values from steady-state measurements were calculated as 1-$I_f(\mathbf{P_6}C_{60})/I_f(\mathbf{P_6})$, where the I_f's are the integrated fluorescence intensities from samples of $\mathbf{P_6}C_{60}$ and $\mathbf{P_6}$ with equal absorbance at the excitation wavelength. The respective Q band region of the absorption spectrum is shown in grey.

Emission Spectra of P_4 and P_4C_{60} at 300 K

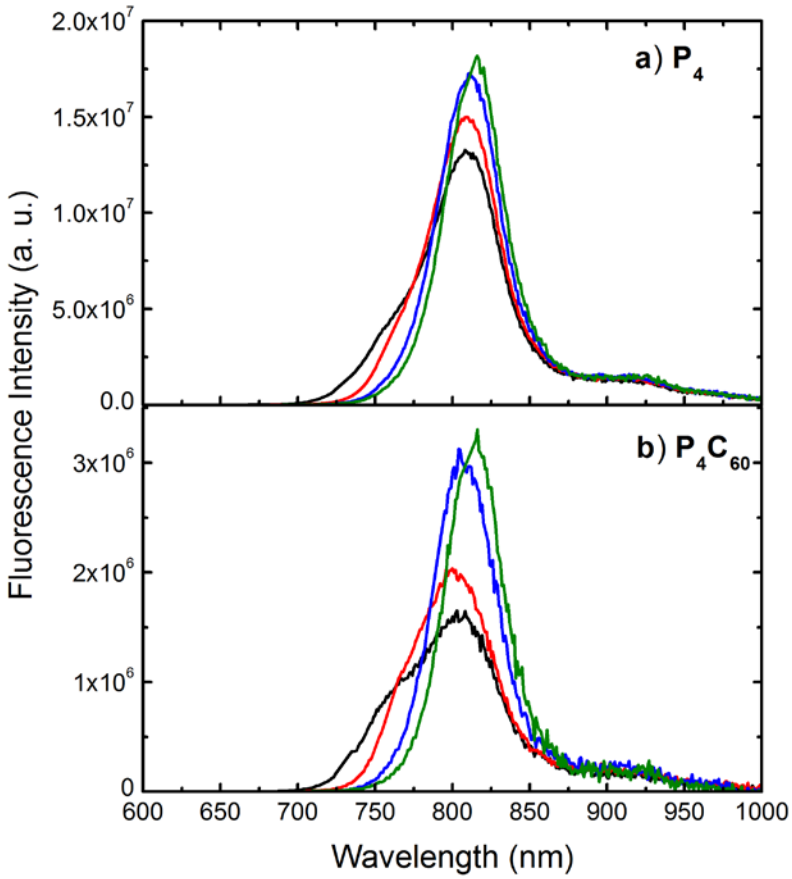

Figure S7. Fluorescence spectra of (a) $\mathbf{P_4}$ and (b) $\mathbf{P_4}C_{60}$ excited at 730 nm (black), 762 nm (red), 790 nm (blue) and 810 nm (green) in 2-MTHF with 1% pyridine added at 300 K. All emission spectra were corrected for the difference in absorbance at the excitation wavelength.

Emission Spectra of P_4-T8 and P_4C_{60}-T8 at 300 K

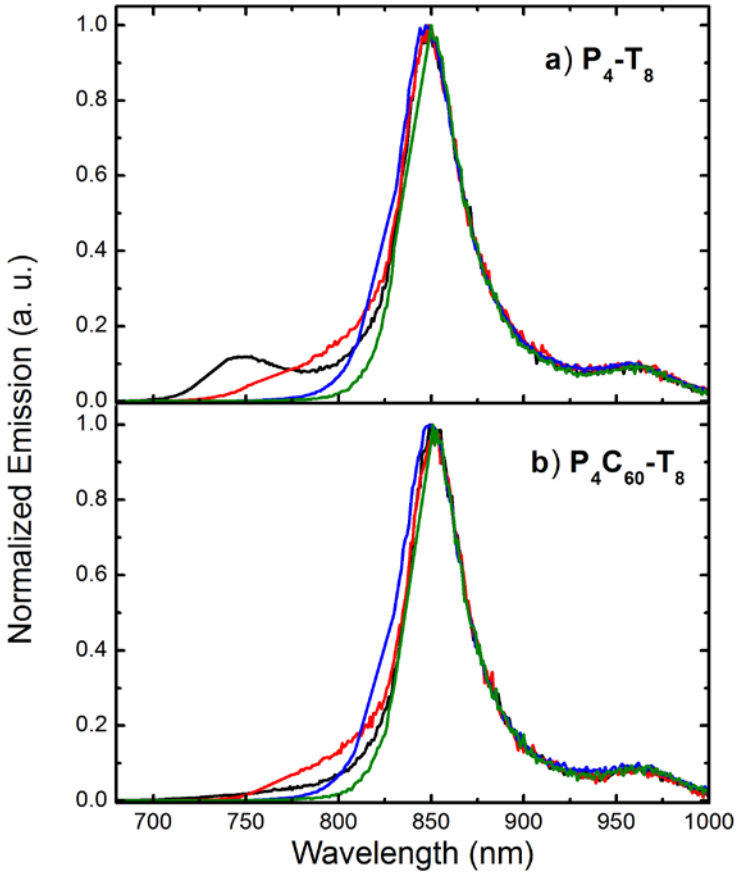

Figure S8. Normalized fluorescence spectra of (a) **P_4-T8** and (b) **P_4C_{60}-T8** excited at 730 nm (black), 765 nm (red), 820 nm (blue) and 840 nm (green) at 300 K in DCM/Toluene (60/40) with 0.1% pyridine added. For both the model and the D-A systems, the small amount of emission visible below 820 nm is due to the presence of free **P_4** and **P_4C_{60}**, respectively. When exciting the model system **P_4-T8** at 730 nm, a second emission peak centered at 750 nm is observed. However no reasonable explanation for this second emission has been found yet.

Emission Spectra of P_6-T8 and P_6C_{60}-T8 at 300 K

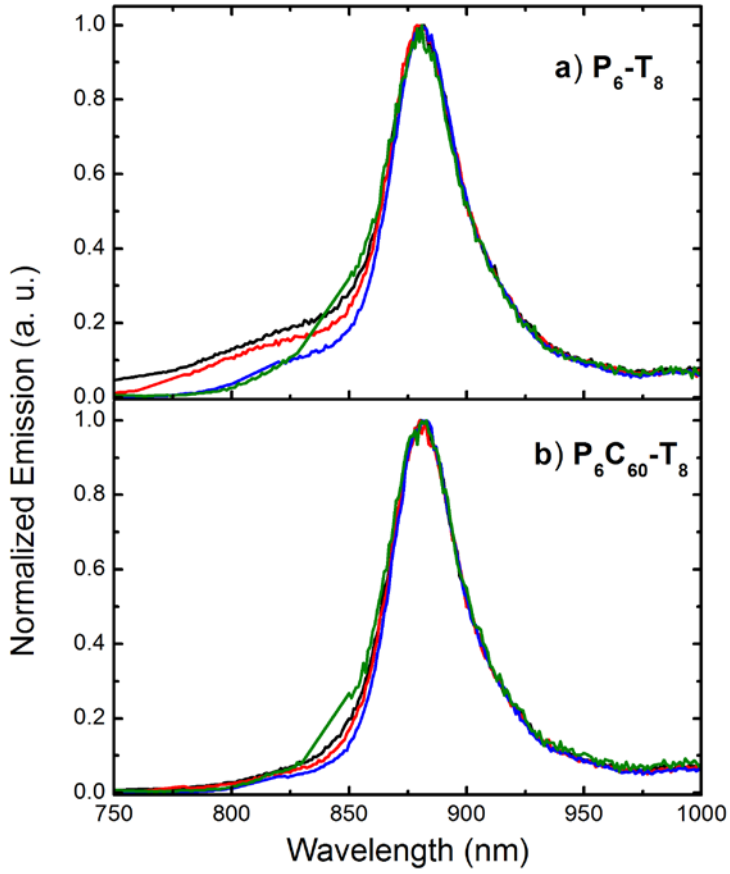

Figure S9. Normalized emission spectra of (a) $\mathbf{P_6}$**-T8** and (b) $\mathbf{P_6}C_{60}$**-T8** excited at 735 nm (black), 772 nm (red), 813 nm (blue) and 843 nm (green) in DCM/Toluene (60/40) with 0.1% pyridine added at 300 K. For all excitation wavelengths, a small amount of emission is visible below 850 nm that resembles the emission of respectively a) free $\mathbf{P_6}$ and b) free $\mathbf{P_6}C_{60}$ with similar excitation spectra. This is therefore attributed to emission from a small amount of free $\mathbf{P_6}$ and $\mathbf{P_6}C_{60}$ still present in solution although the ligand **T8** is present in large excess. The effect of free $\mathbf{P_6}C_{60}$ is less evident due to the relative strong quenching (~50%) of the donor $\mathbf{P_6}$ in the linear compound $\mathbf{P_6}C_{60}$.

Quantum Yield for Charge Separation of P_6C_{60} in DCM/Toluene

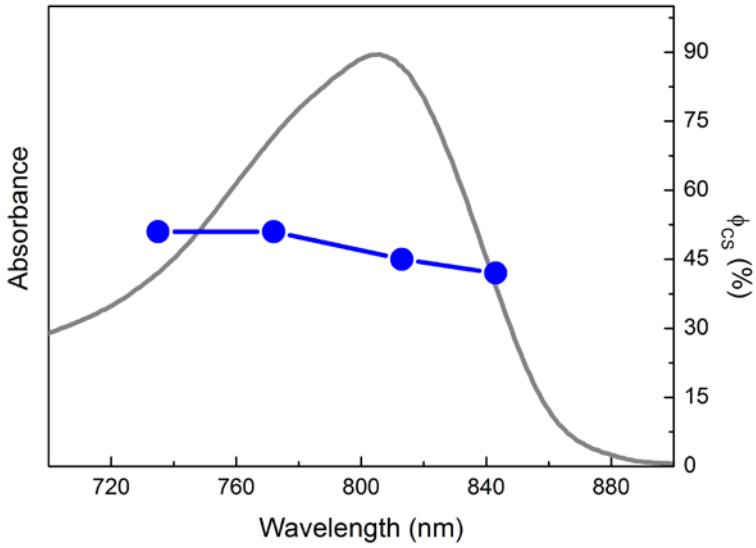

Figure S10. Quantum yield for charge separation as function of the excitation wavelength for $\mathbf{P_6}C_{60}$ in DCM/Toluene (60/40) with 0.1% pyridine added based on steady-state measurements at 300 K. The values from steady-state measurements were calculated as $1-I_f(\mathbf{P_6}C_{60})/I_f(\mathbf{P_6})$, where the I_f's are the integrated fluorescence intensities from samples of $\mathbf{P_6}C_{60}$ and $\mathbf{P_6}$ with equal absorbance at the excitation wavelength. The respective Q band region of the absorption spectrum is shown in grey.

Singular Value Decomposition

Singular value decomposition (SVD) is a general mathematical tool to factorize a rectangular matrix in matrices of orthogonal components. If **A** is the set of time dependent transient absorption spectra arranged into a rectangular *n*x*m* matrix (*n* wavelengths points and *m* time points) this matrix may be decomposed according to:

$$\mathbf{A} = \mathbf{U}\mathbf{S}\mathbf{V}^{\mathbf{T}} \qquad (1)$$

where **U** is a *n*x*n* matrix consisting of the orthogonal component "spectra", **V** is a *m*x*m* matrix consisting of the orthogonal "time profiles" and **S** is a diagonal *n*x*m* matrix containing the positive singular values in decreasing magnitude along the diagonal. At this point SVD is just a powerful tool to extract the number of relevant components in a set of measurements. This is done by either comparing the singular values or by inspecting the orthogonal components and try to judge how many of them contain actual spectral information. In a typical application many hundreds of spectra are measured (varying the delay time) but only a few components are needed to describe the entire dataset. By only retaining those that contain actual information, SVD effectively reduces the noise. More importantly, this procedure give the number of independent components which is the minimum information needed for creating a kinetic model. If we have *k* independent components, the matrix **A** could be approximately described by

$$\mathbf{A} = \mathbf{U}^{\mathbf{red}}\mathbf{V}^{\mathbf{red}} \qquad (2)$$

where $\mathbf{U}^{\mathbf{red}}$ is a *n*x*k* matrix and $\mathbf{V}^{\mathbf{red}}$ is a *k*x*m* matrix containing only the *k* relevant orthogonal component spectra and corresponding time profiles, respectively.

In order to get physically meaningful component spectra and time profiles from the orthogonal components we need to have a physical condition (the number of possible decompositions according to Eq. 1 is infinite) that connect the different components. In the case at hand we know that the real components are related via the kinetic scheme and so it should be possible to relate their variation in concentration with time to the measured variation of the spectra (through optimized rate constants). In compact mathematical form the $\mathbf{U}^{\mathbf{red}}$ and $\mathbf{V}^{\mathbf{red}}$ matrices are related through matrix rotation to the true spectral and time dependent concentration matrices, **T** and **C**, respectively:

$$\mathbf{U}^{red} = \mathbf{T}\mathbf{R}^{-1} \text{ and } \mathbf{V}^{red} = \mathbf{R}\mathbf{C} \qquad (3)$$

where **R** is a small square *k*x*k* rotation matrix.

In practice the concentration matrix (**C**) is found through non-linear optimization of the rate constants minimizing the least square difference between the measured spectral matrix and the simulated one, i.e. forming the appropriate norm ||**A – TC**|| and searching for its minimum. Since all photophysical processes are assumed to be first order, **C** is found as the solution to the master equation d**C**/dt=**kC** where **k** is a matrix of the relevant combination of rate constants.

The procedure is: (1) Find the number of independent components through SVD, (2) Make a kinetic model which is consistent with the number of emissive components (in this case, 2 or 3 depending on excitation wavelength) and any other general knowledge of the system (e.g. initial excitation conditions). This is a crucial step since in general many different models might be consistent with a given number of components. (3) Derive the matrix **k** from the model and do the non-linear optimization. In this way the optimized rate constants (and therefore the time dependent concentrations) and the spectral shapes of the contributing components are found.

Table S1. Wavelength Dependence of the rate constants related to the planarization and natural decays of both systems studied P_4 and P_6 at 300 K

λ_{exc} / nm	P_4 / P_4C_{60}			λ_{exc} / nm	P_6 / P_6C_{60}		
	$k^{a)}$ /10^9 s^{-1}	k_1 /10^9 s^{-1}	k_2 /10^9 s^{-1}		$k^{a)}$ /10^9 s^{-1}	k_1 /10^9 s^{-1}	k_2 /10^9 s^{-1}
730	1.6	4.0	3.8	730	1.5	5.2	5.3
760	2.0	2.8	2.7	780	1.5	8.1	0.7
790	1.6	-	4.3	820	1.9	-	6.5
810	1.6	-	2.5	840	1.5	-	4.9

a) The results presented in the table were obtained with the assumption $k = k^{\#} = k^{¤} = k^*$, i. e. the fluorescence decay rates (i. e. radiative rate + non-radiative rate) were weakly dependent on the conformational states.

Table S2. Wavelength Dependence of the rate constants related to the planarization, natural decays and charge separation of P_6C_{60} at 180 K

λ_{exc} / nm	P_6C_{60}					
	k_f /10^9 s^{-1}	k_1 /10^9 s^{-1}	k_2 /10^9 s^{-1}	$k_{cs}^{\#}$ /10^9 s^{-1}	$k_{cs}^{¤}$ /10^9 s^{-1}	k_{cs}^{*} /10^9 s^{-1}
730	1.1	2.1	1.2	0.9	0.5	0.2
780	1.9	0.9	0.6	2.6	0.7	0.0
820	1.5	-	1.6	-	1.8	0.1
840	1.6	-	0.6	-	1.2	0.0

Table S3. Extracted fluorescence lifetimes of the reference systems P_6 and P_4 at 300 K

P_4				P_6			
λ_{exc} /nm	Lifetimes			λ_{exc} /nm	Lifetimes		
	τ_1/ps	τ_2/ps	τ_3/ps		τ_1/ps	τ_2/ps	τ_3/ps
730	179	187	640	730	148	147	665
760	210	211	497	780	104	446	667
790	-	168	611	820	-	118	524
810	-	241	622	840	-	148	541

Table S4. Extracted Lifetimes of P_6C_{60} and P_4C_{60} as function of the excitation wavelength at 300 K.

P_4C_{60}				P_6C_{60}			
λ_{exc} / nm	Lifetimes*			λ_{exc} / nm	Lifetimes*		
	τ_1 / ps	τ_2 / ps	τ_3 / ps		τ_1 / ps	τ_2/ps	τ_3 / ps
730	53	125	402	730	65	147	559
760	51	134	497	780	55	198	501
790	-	75	316	820	-	86	409
810	-	99	444	840	-	156	422

*The lifetimes were calculated as $\tau_1=1/(k^{\#}+k_1+k_{cs}^{\#})$, $\tau_2=1/(k^{¤}+k_2+k_{cs}^{¤})$, $\tau_3=1/(k^{*}+k_{cs}^{*})$ respectively.

Table S5. Extracted fluorescence lifetimes of P_6 and P_6C_{60} at 180 K

P_6				P_6C_{60}			
λ_{exc} /nm	Lifetimes			λ_{exc} /nm	Lifetimes		
	τ_1/ps	τ_2/ps	τ_3/ps		τ_1/ps	τ_2/ps	τ_3/ps
730	311	425	876	730	245	364	802
780	357	402	539	780	185	317	525
820	-	325	679	820	-	205	625
840	-	439	610	840	-	292	610

*The lifetimes were calculated as $\tau_1=1/(k^{\#}+k_1+k_{cs}^{\#})$, $\tau_2=1/(k^{¤}+k_2+k_{cs}^{¤})$, $\tau_3=1/(k^{*}+k_{cs}^{*})$ respectively.

Analysis of 2D streak camera images of P_6 emission at 300 K

- ***Excitation at 730 nm***

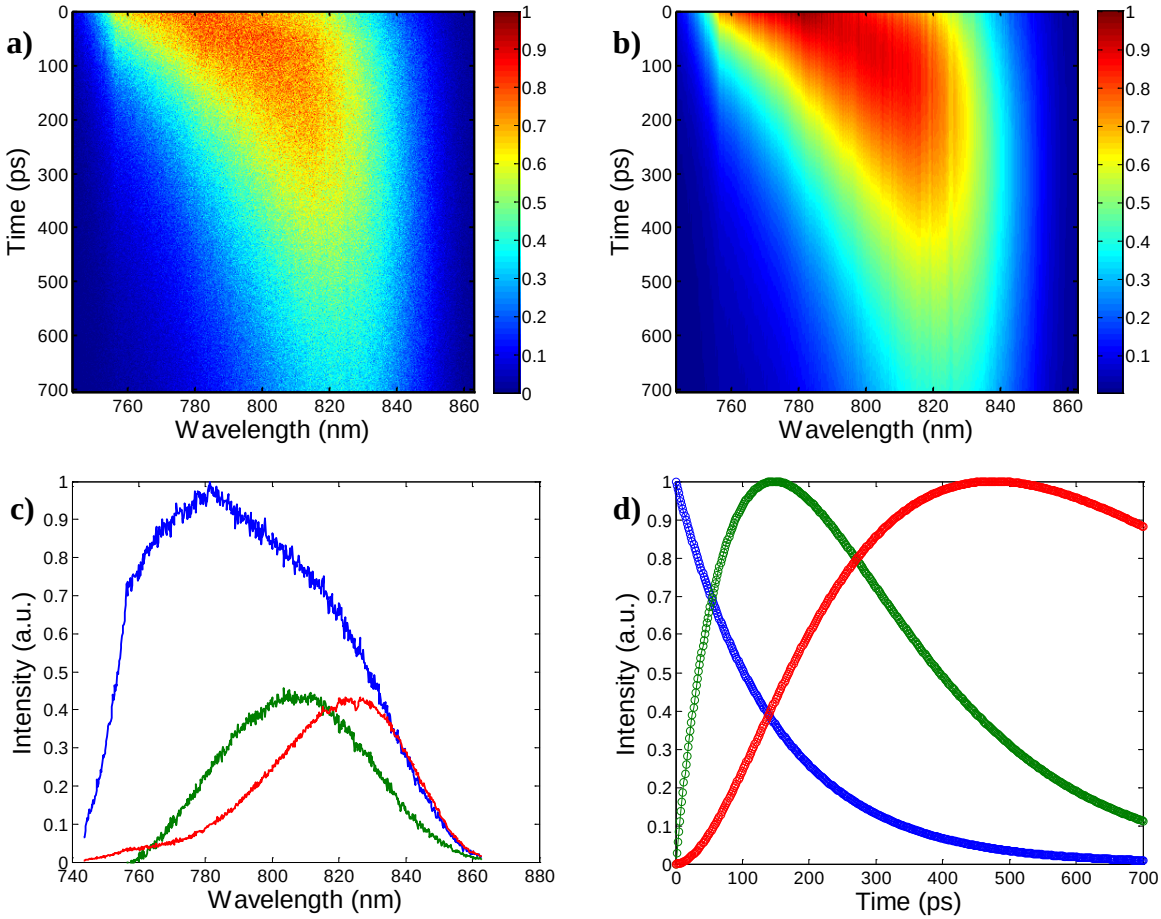

Figure S11. a) Normalized 2D streak camera image of the emission of $\mathbf{P_6}$ excited at 730 nm at 300 K in 2-MTHF with 1% pyridine. b) Reconstructed 2D image of the emission of $\mathbf{P_6}$ excited at 730 nm. This image was built from data obtained in the fitting procedure. c) Spectral components and d) fluorescence decays of the 3 species contributing to the fluorescence emission. The color code used in c) and d) is the same, i.e. the fluorescence decay in blue corresponds to the species with the blue emission etc.

- ***Excitation at 780 nm***

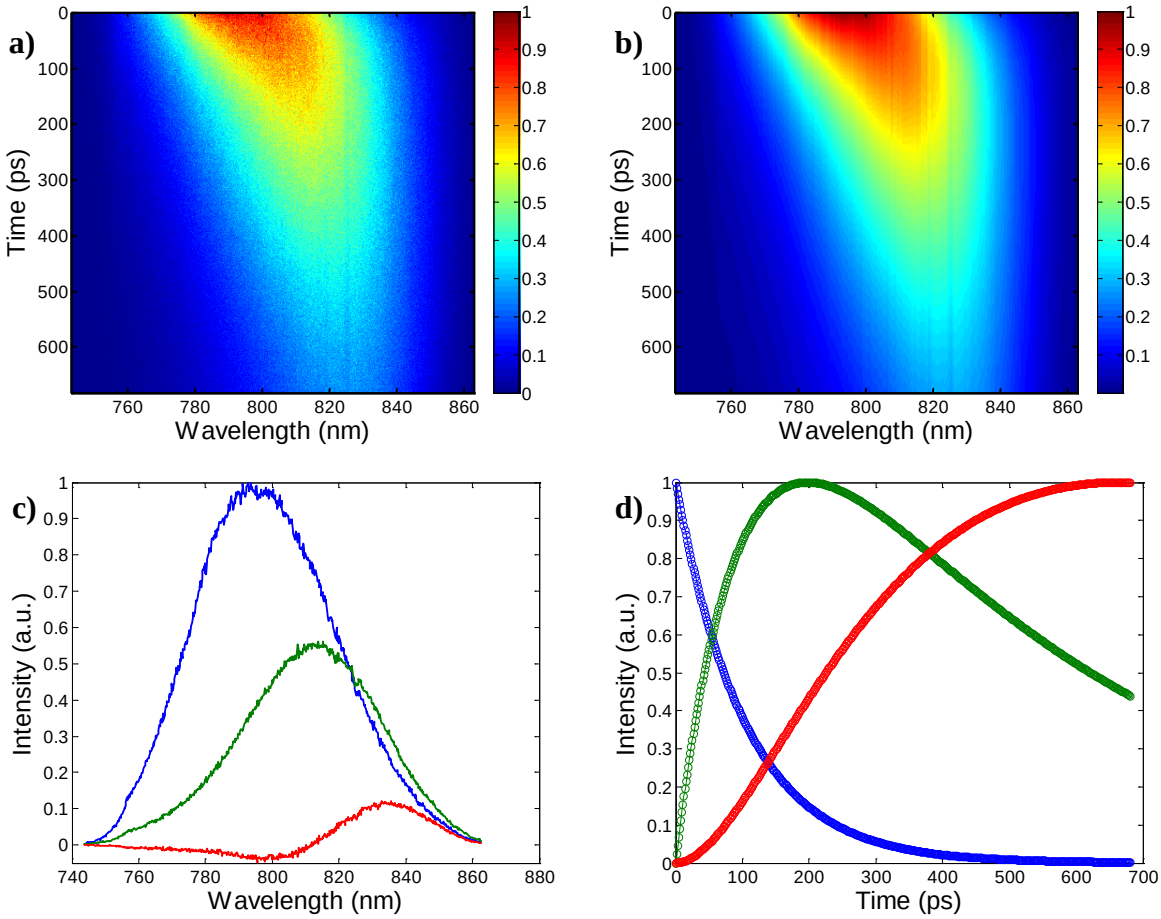

Figure S12. a) Normalized 2D streak camera image of the emission of $\mathbf{P_6}$ excited at 780 nm at 300 K in 2-MTHF with 1% pyridine. b) Reconstructed 2D image of the emission of $\mathbf{P_6}$ excited at 780 nm. This image was built from data obtained in the fitting procedure. c) Spectral components and d) fluorescence decays of the 3 species contributing to the fluorescence emission. The color code used in c) and d) is the same, i.e. the fluorescence decay in blue corresponds to the species with the blue emission etc.

- ***Excitation at 820 nm***

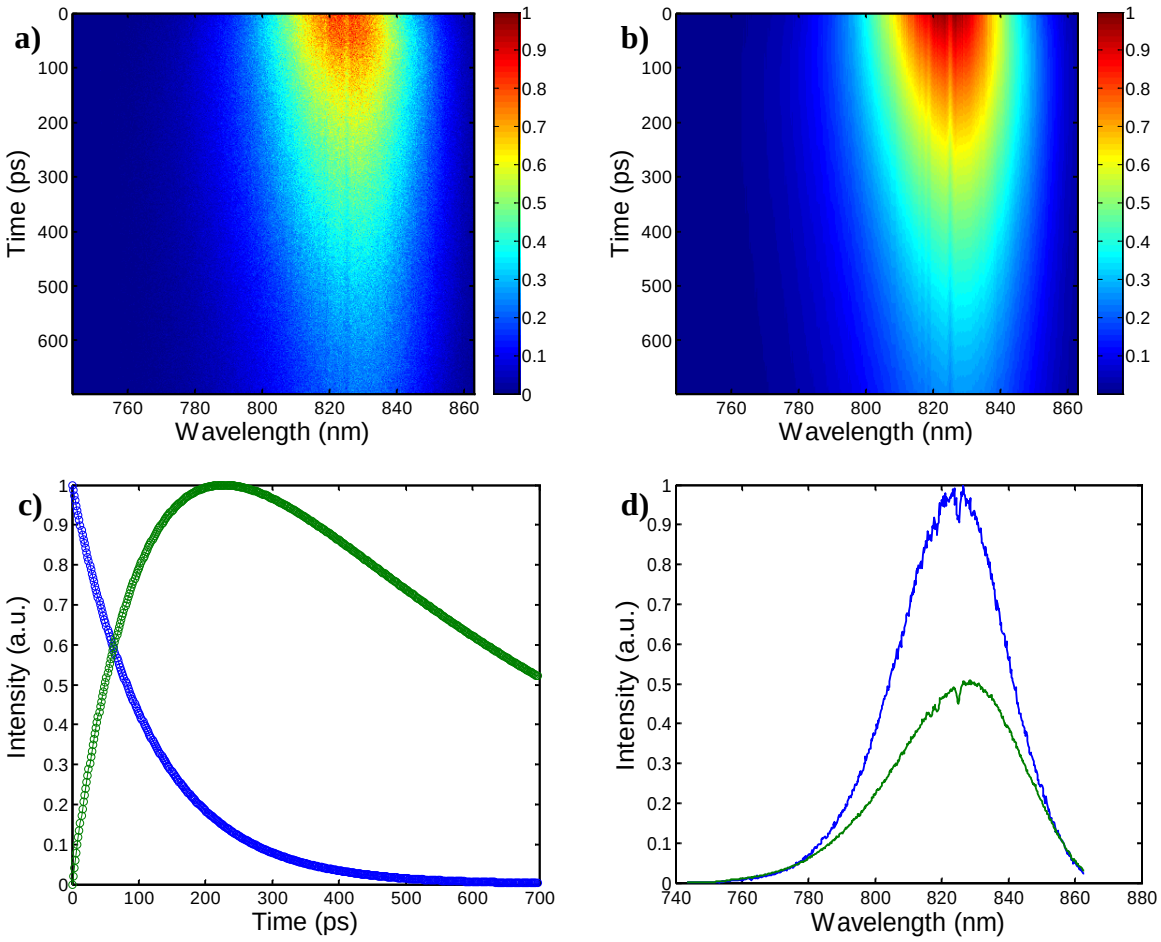

Figure S13. a) Normalized 2D streak camera image of the emission of $\mathbf{P_6}$ excited at 820 nm at 300 K in 2-MTHF with 1% pyridine. b) Reconstructed 2D image of the emission of $\mathbf{P_6}$ excited at 820 nm. This image was built from data obtained in the fitting procedure. c) Spectral components and d) fluorescence decays of the 2 species contributing to the fluorescence emission. The color code used in c) and d) is the same, i.e. the fluorescence decay in blue corresponds to the species with the blue emission etc.

- ***Excitation at 840 nm***

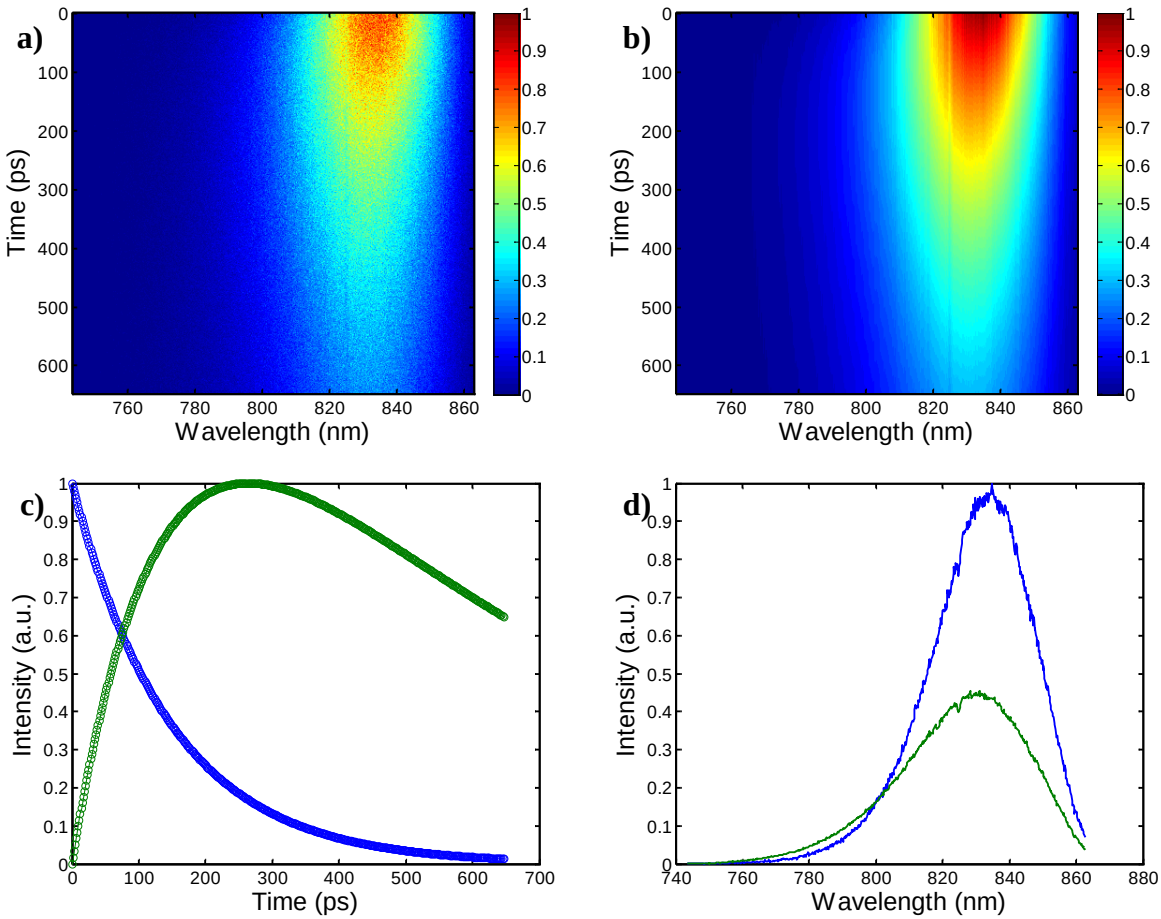

Figure S14. a) Normalized 2D streak camera image of the emission of $\mathbf{P_6}$ excited at 840 nm at 300 K in 2-MTHF with 1% pyridine. b) Reconstructed 2D image of the emission of $\mathbf{P_6}$ excited at 840 nm. This image was built from data obtained in the fitting procedure. c) Spectral components and d) fluorescence decays of the 2 species contributing to the fluorescence emission. The color code used in c) and d) is the same, i.e. the fluorescence decay in blue corresponds to the species with the blue emission etc.

Analysis of 2D streak camera images of P_6C_{60} emission at 300 K

- ***Excitation at 780 nm***

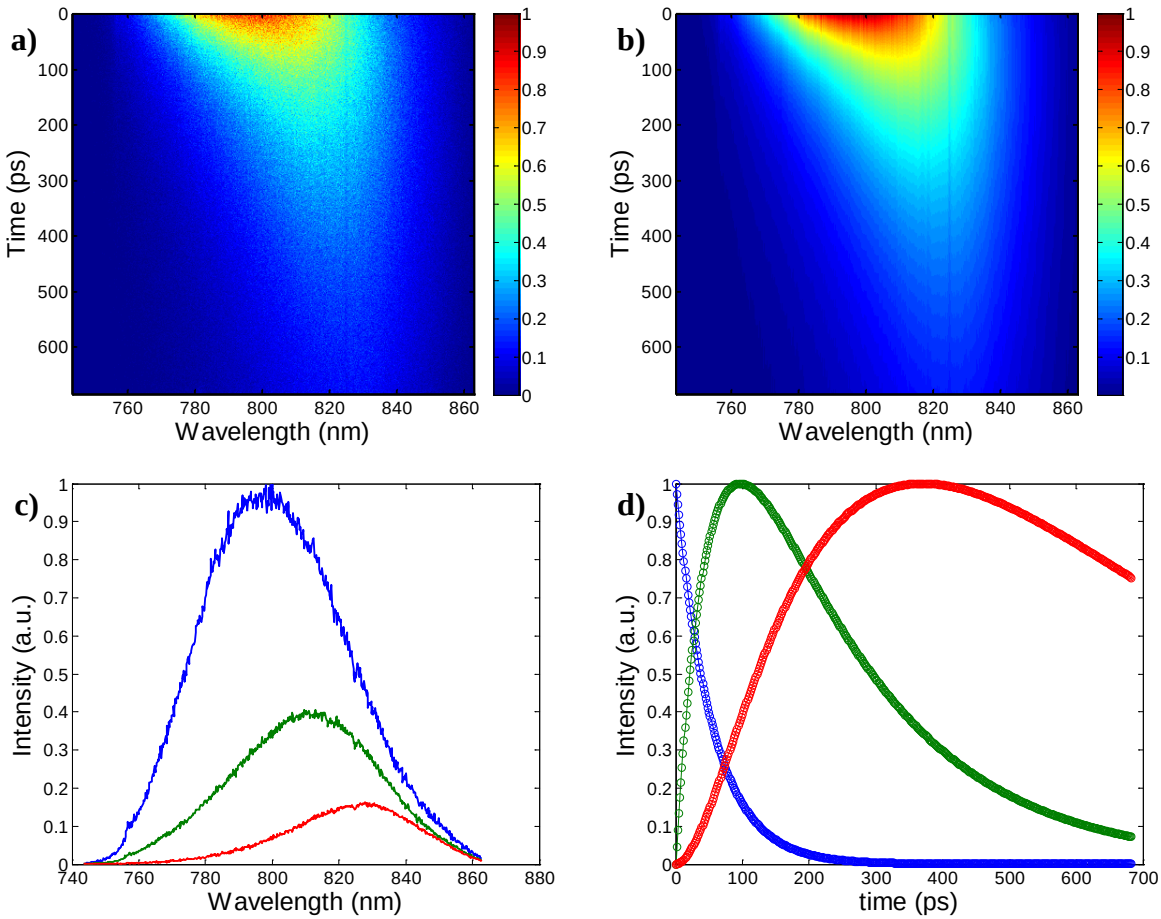

Figure S15. a) Normalized 2D streak camera image of the emission of $\mathbf{P_6}C_{60}$ excited at 780 nm at 300 K in 2-MTHF with 1% pyridine. b) Reconstructed 2D image of the emission of $\mathbf{P_6}C_{60}$ excited at 780 nm. This image was built from data obtained in the fitting procedure. c) Spectral components and d) fluorescence decays of the 3 species contributing to the fluorescence emission. The color code used in c) and d) is the same, i.e. the fluorescence decay in blue corresponds to the species with the blue emission etc.

- ***Excitation at 820 nm***

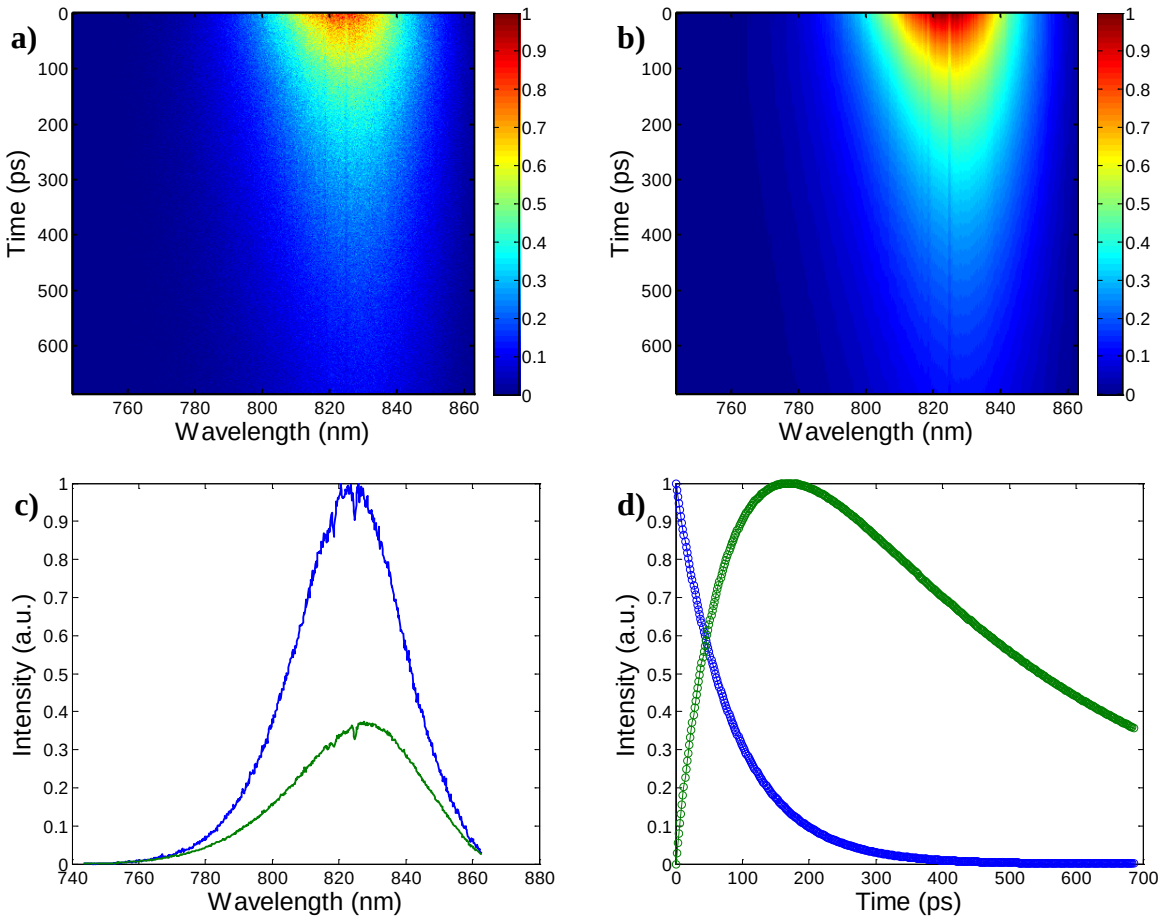

Figure S16. a) Normalized 2D streak camera image of the emission of $\mathbf{P_6}C_{60}$ excited at 820 nm at 300 K in 2-MTHF with 1% pyridine. b) Reconstructed 2D image of the emission of $\mathbf{P_6}C_{60}$ excited at 820 nm. This image was built from data obtained in the fitting procedure. c) Spectral components and d) fluorescence decays of the 2 species contributing to the fluorescence emission. The color code used in c) and d) is the same, i.e. the fluorescence decay in blue corresponds to the species with the blue emission etc.

- ***Excitation at 840 nm***

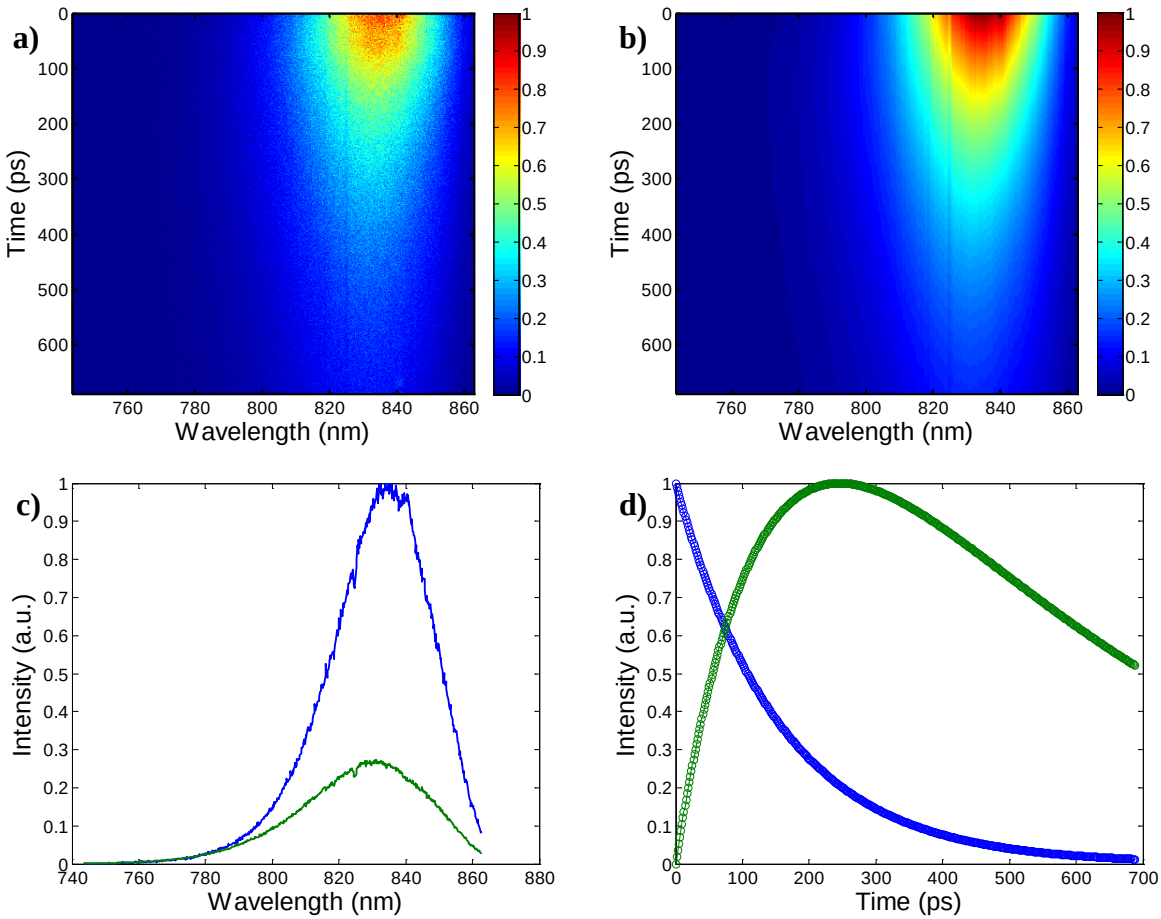

Figure S17. a) Normalized 2D streak camera image of the emission of $\mathbf{P_6}C_{60}$ excited at 840 nm at 300 K in 2-MTHF with 1% pyridine. b) Reconstructed 2D image of the emission of $\mathbf{P_6}C_{60}$ excited at 840 nm. This image was built from data obtained in the fitting procedure. c) Spectral components and d) fluorescence decays of the 2 species contributing to the fluorescence emission. The color code used in c) and d) is the same, i.e. the fluorescence decay in blue corresponds to the species with the blue emission etc.

Analysis of 2D streak camera images of P_4 at 300 K

- ***Excitation at 730 nm***

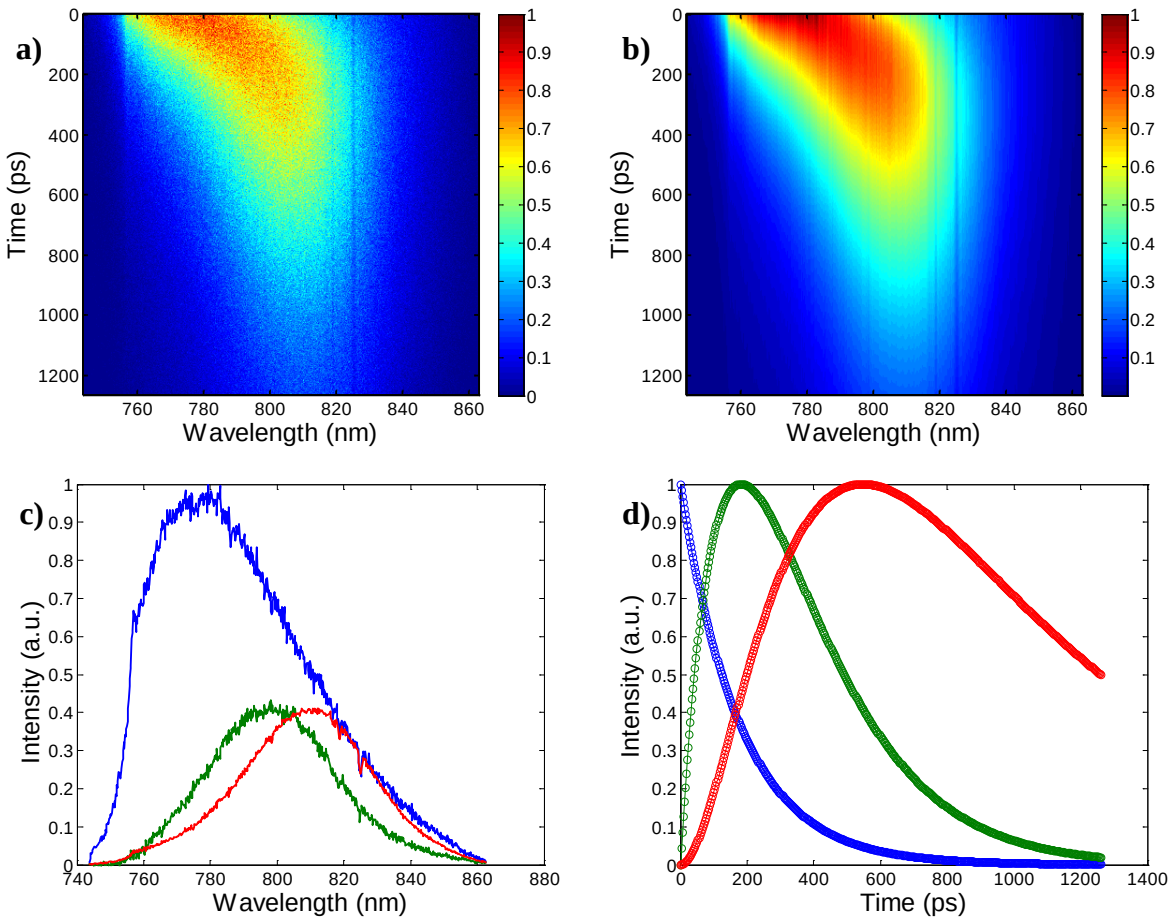

Figure S18. a) Normalized 2D streak camera image of the emission of $\mathbf{P_4}$ excited at 730 nm at 300 K in 2-MTHF with 1% pyridine. b) Reconstructed 2D image of the emission of $\mathbf{P_4}$ excited at 730 nm. This image was built from data obtained in the fitting procedure. c) Spectral components and d) fluorescence decays of the 3 species contributing to the fluorescence emission. The color code used in c) and d) is the same, i.e. the fluorescence decay in blue corresponds to the species with the blue emission etc.

- ***Excitation at 760 nm***

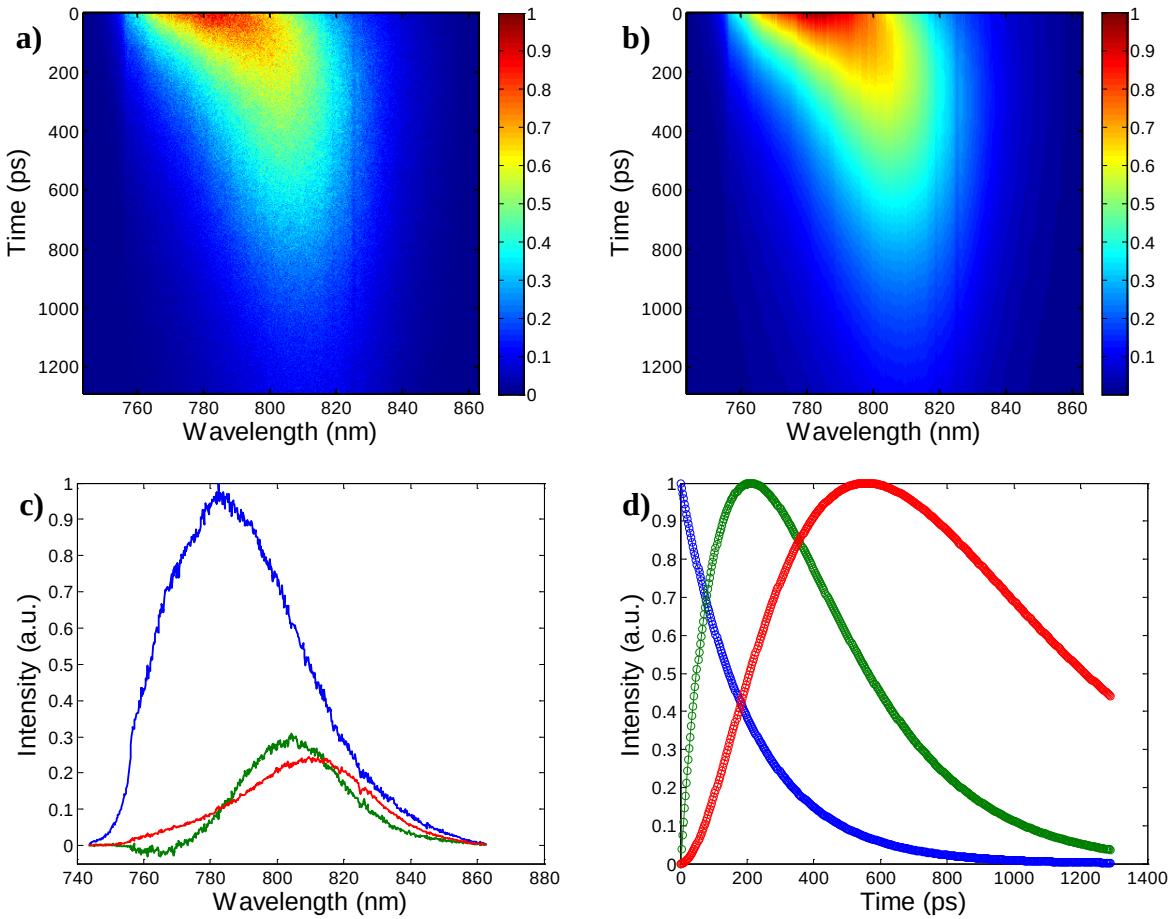

Figure S19. a) Normalized 2D streak camera image of the emission of $\mathbf{P_4}$ excited at 760 nm at 300 K in 2-MTHF with 1% pyridine; b) Reconstructed 2D image of the emission of $\mathbf{P_4}$ excited at 760 nm. This image was built from data obtained in the fitting procedure; c) Spectral components and d) fluorescence decays of the 3 species contributing to the fluorescence emission. The color code used in c) and d) is the same, i.e. the fluorescence decay in blue corresponds to the species with the blue emission etc.

- ***Excitation at 790 nm***

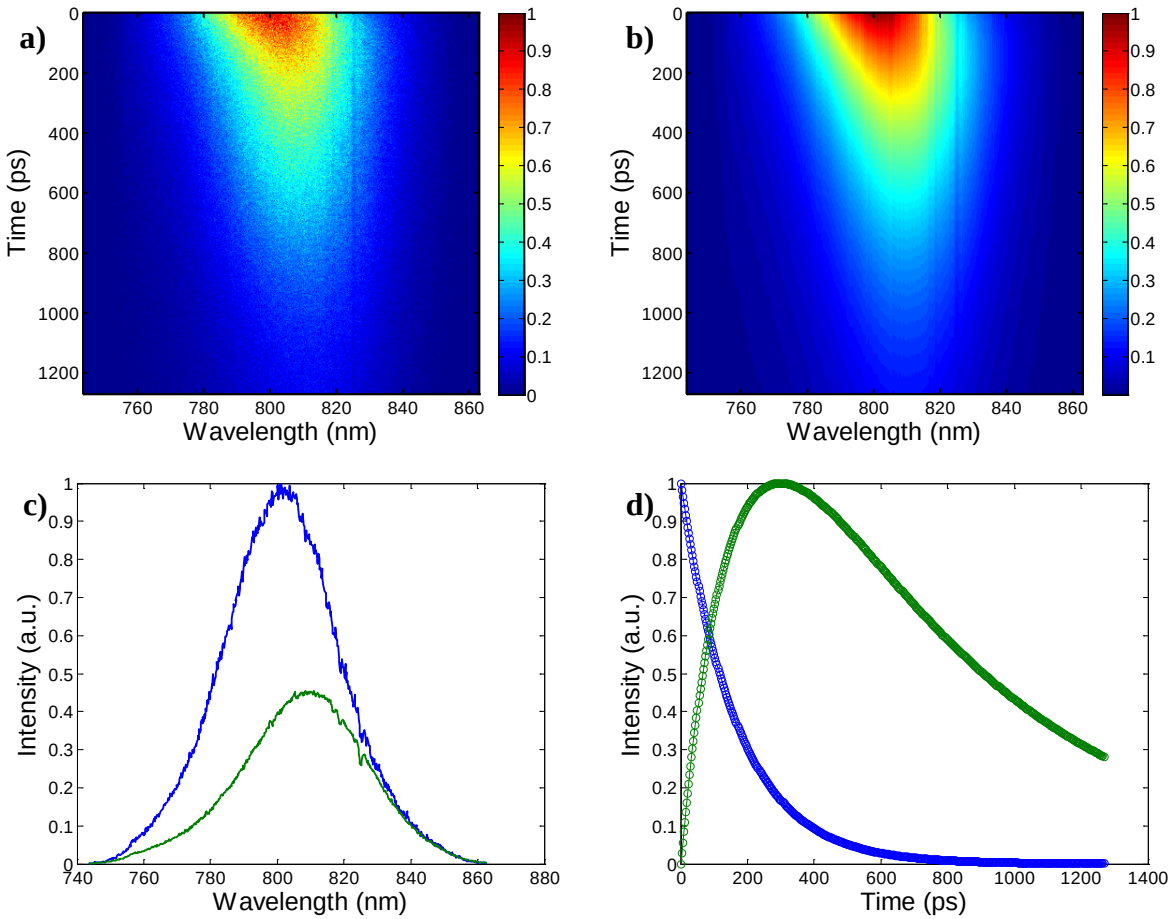

Figure S20. a) Normalized 2D streak camera image of the emission of $\mathbf{P_4}$ excited at 790 nm at 300 K in 2-MTHF with 1% pyridine; b) Reconstructed 2D image of the emission of $\mathbf{P_4}$ excited at 790 nm. This image was built from data obtained in the fitting procedure; c) Spectral components and d) fluorescence decays of the 2 species contributing to the fluorescence emission. The color code used in c) and d) is the same, i.e. the fluorescence decay in blue corresponds to the species with the blue emission etc.

- ***Excitation at 810 nm***

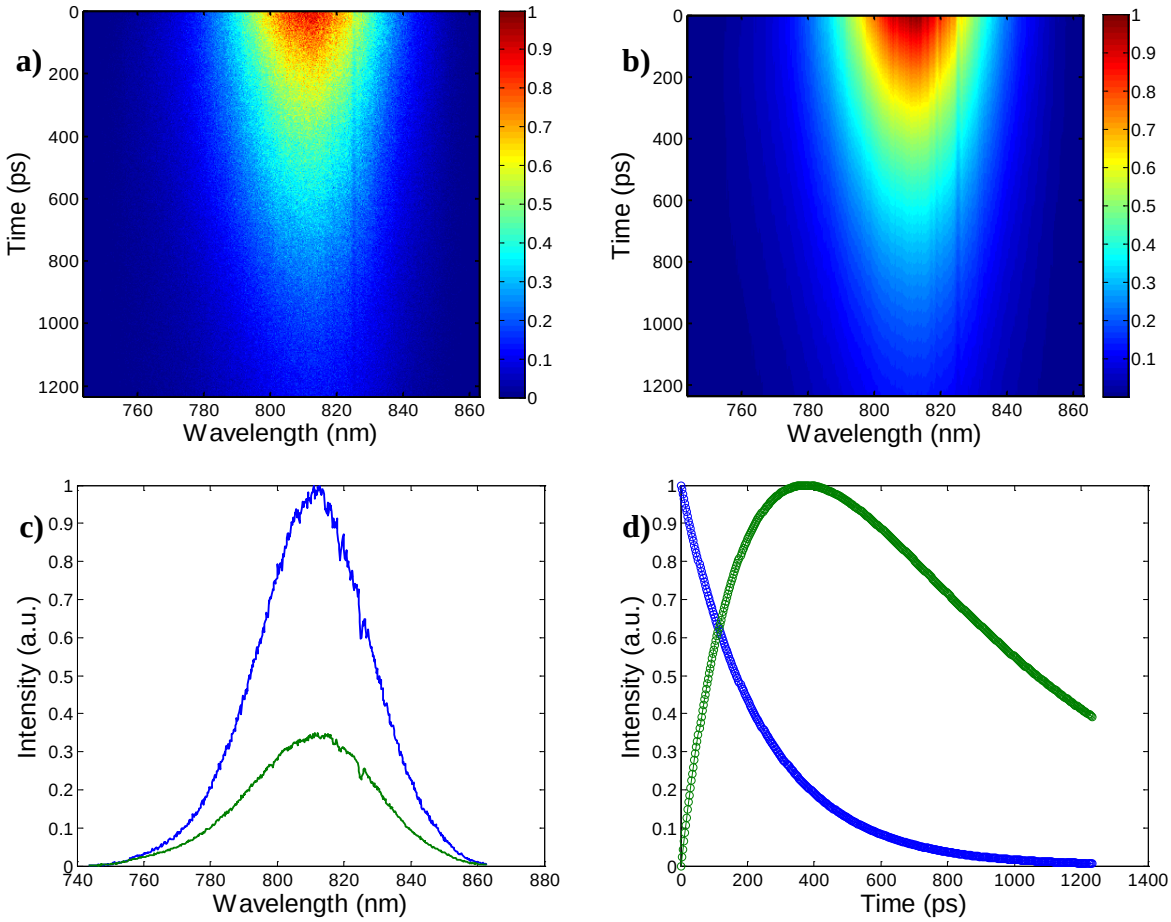

Figure S21. a) Normalized 2D streak camera image of the emission of $\mathbf{P_4}$ excited at 810 nm at 300 K in 2-MTHF with 1% pyridine. b) Reconstructed 2D image of the emission of $\mathbf{P_4}$ excited at 810 nm. This image was built from data obtained in the fitting procedure. c) Spectral components and d) fluorescence decays of the 2 species contributing to the fluorescence emission. The color code used in c) and d) is the same, i.e. the fluorescence decay in blue corresponds to the species with the blue emission etc.

Analysis of 2D streak camera images of P_4C_{60} at 300 K

- ***Excitation at 730 nm***

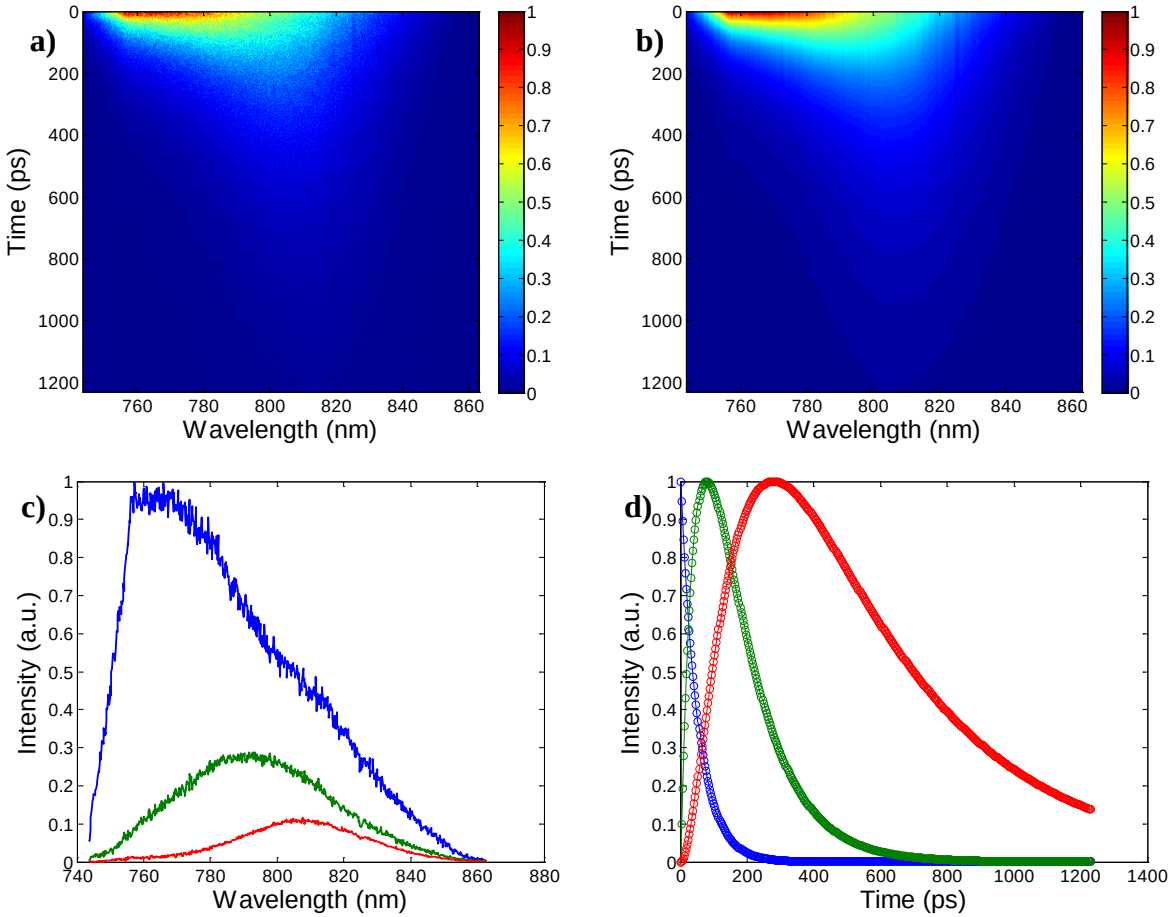

Figure S22. a) Normalized 2D streak camera images of the emission of $\mathbf{P_4}C_{60}$ excited at 730 nm at 300 K in 2-MTHF with 1% pyridine. b) Reconstructed 2D image of the emission of $\mathbf{P_4}C_{60}$ excited at 730 nm. This image was built from data obtained in the fitting procedure. c) Spectral components and d) fluorescence decays of the 3 species contributing to the fluorescence emission. The color code used in c) and d) is the same, i.e. the fluorescence decay in blue corresponds to the species with the blue emission etc.

- ***Excitation at 760 nm***

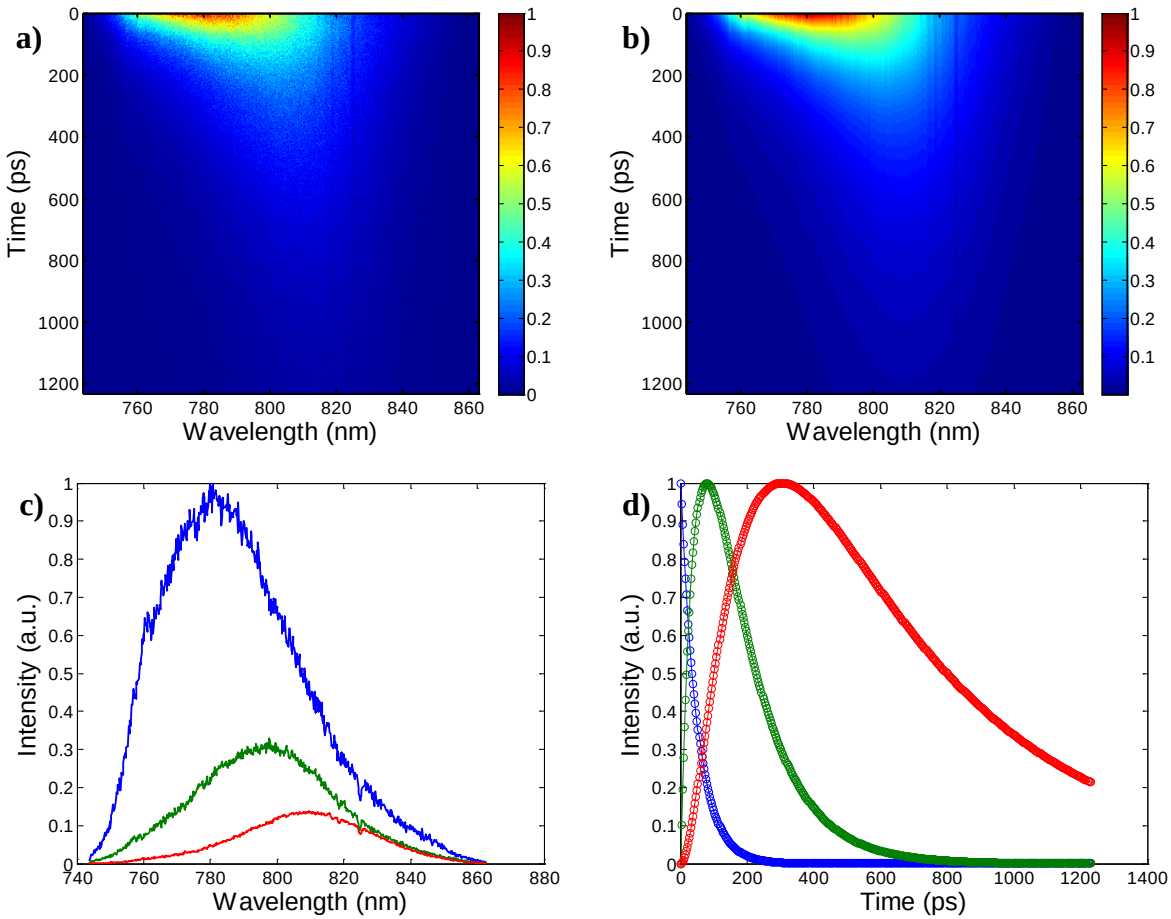

Figure S23. a) Normalized 2D streak camera image of the emission of $\mathbf{P_4}C_{60}$ excited at 760 nm at 300 K in 2-MTHF with 1% pyridine. b) Reconstructed 2D image of the emission of $\mathbf{P_4}C_{60}$ excited at 760 nm. This image was built from data obtained in the fitting procedure. c) Spectral components and d) fluorescence decays of the 3 species contributing to the fluorescence emission. The color code used in c) and d) is the same, i.e. the fluorescence decay in blue corresponds to the species with the blue emission etc.

- ***Excitation at 790 nm***

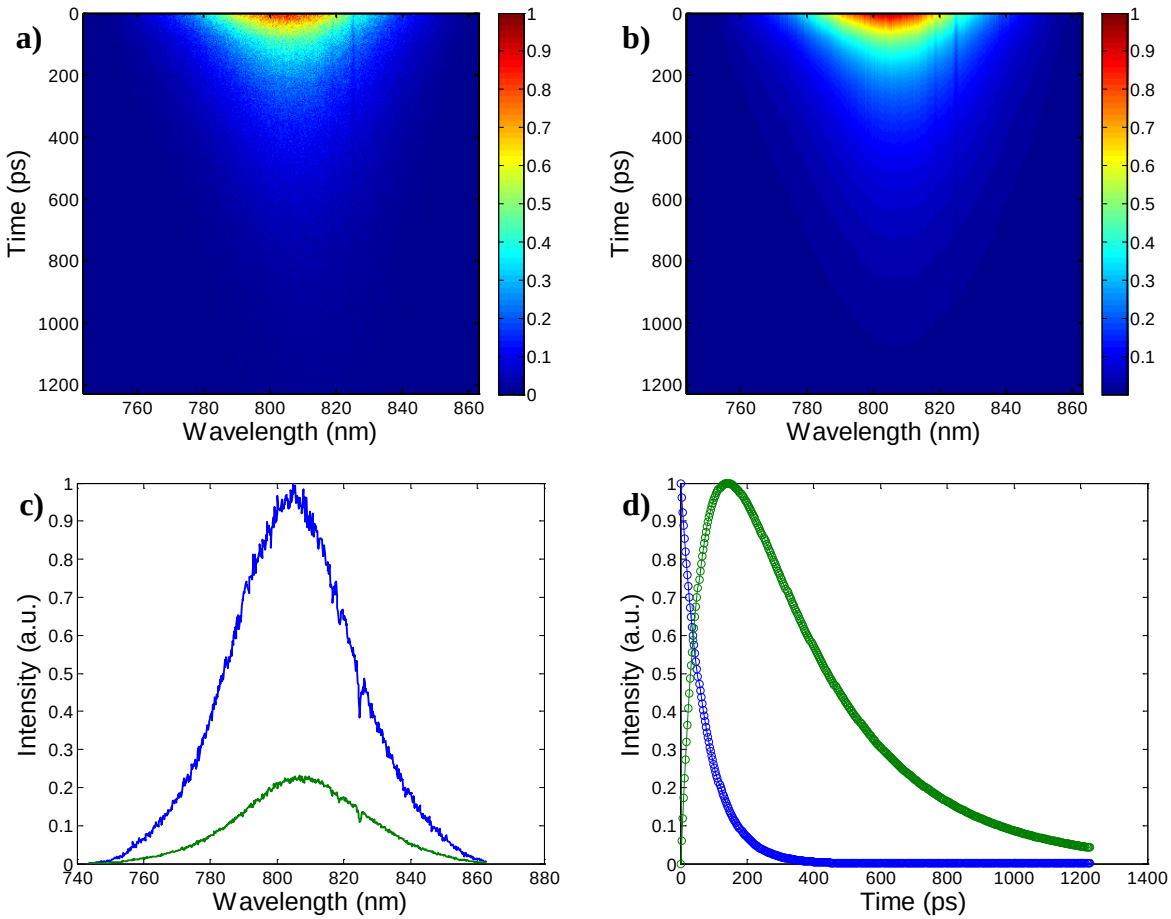

Figure S24. a) Normalized 2D streak camera image of the emission of $\mathbf{P_4}C_{60}$ excited at 790 nm at 300 K in 2-MTHF with 1% pyridine. b) Reconstructed 2D image of the emission of $\mathbf{P_4}C_{60}$ excited at 790 nm. This image was built from data obtained in the fitting procedure. c) Spectral components and d) fluorescence decays of the 2 species contributing to the fluorescence emission. The color code used in c) and d) is the same, i.e. the fluorescence decay in blue corresponds to the species with the blue emission etc.

- ***Excitation at 810 nm***

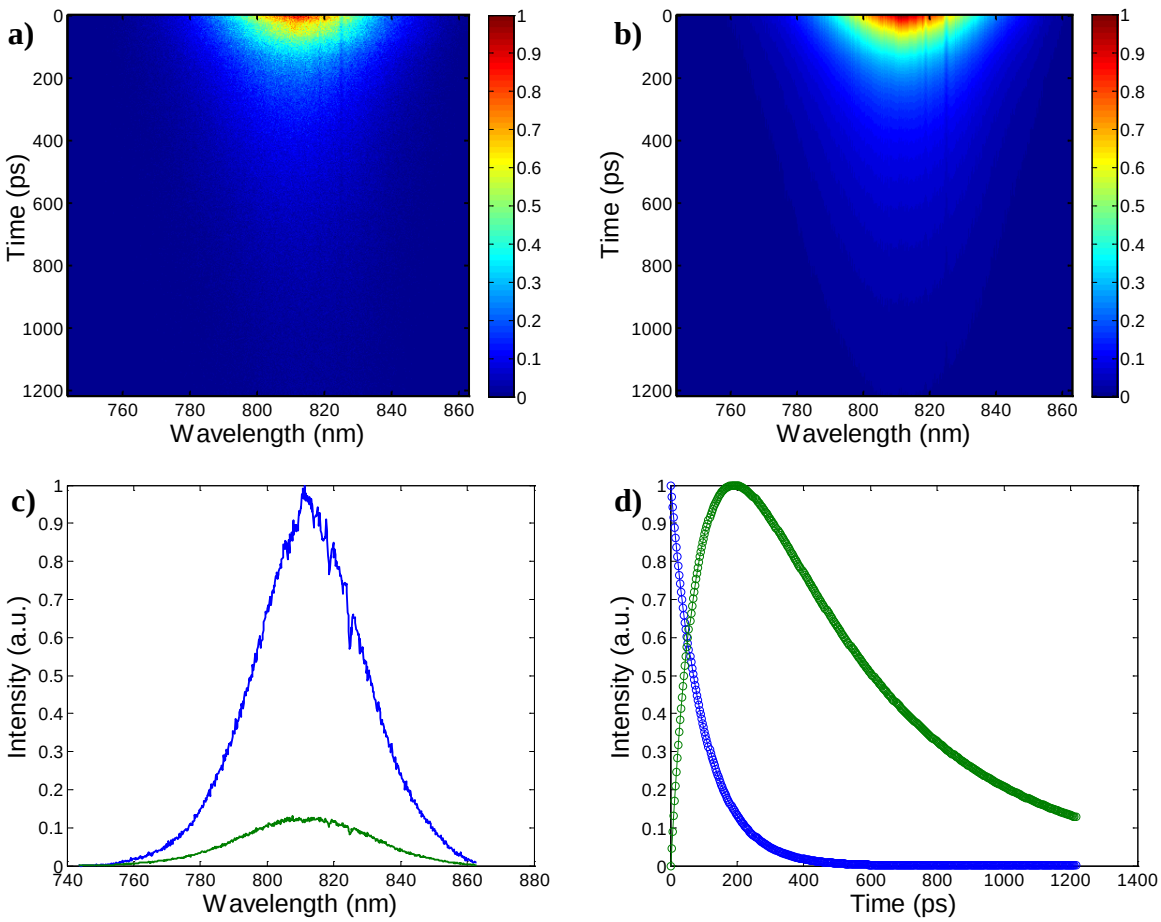

Figure S25. a) 2D streak camera image of the emission of $\mathbf{P_4}C_{60}$ excited at 810 nm at 300 K in 2-MTHF with 1% pyridine. b) Reconstructed 2D image of the emission of $\mathbf{P_4}C_{60}$ excited at 810 nm. This image was built from data obtained in the fitting procedure. c) Spectral components and d) fluorescence decays of the 2 species contributing to the fluorescence emission. The color code used in c) and d) is the same, i.e. the fluorescence decay in blue corresponds to the species with the blue emission etc.

Analysis of 2D streak camera images of P_6 emission at 180 K

- ***Excitation at 730 nm***

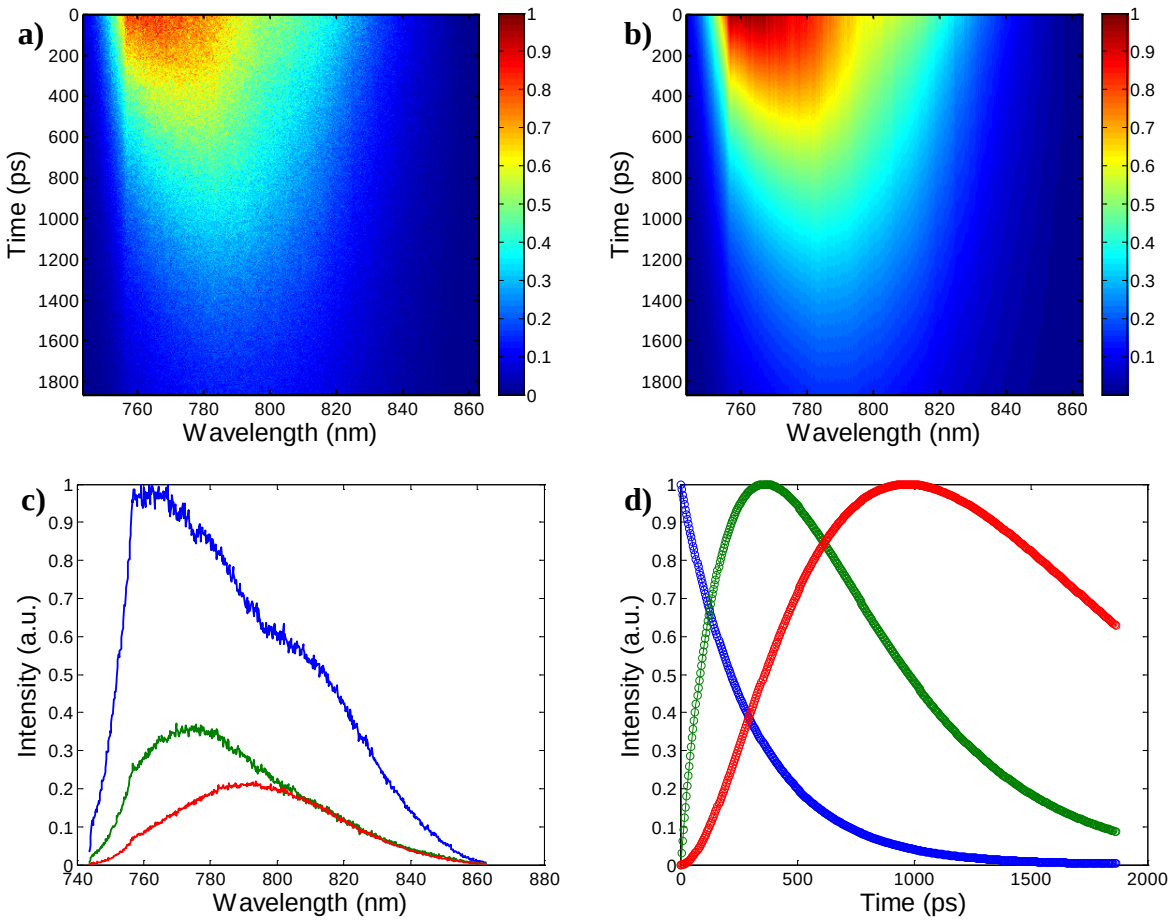

Figure S26. a) Normalized 2D streak camera image of the emission of $\mathbf{P_6}$ excited at 730 nm at 180 K in 2-MTHF with 1% pyridine. b) Reconstructed 2D image of the emission of $\mathbf{P_6}$ excited at 840 nm. This image was built from data obtained in the fitting procedure. c) Spectral components and d) fluorescence decays of the 3 species contributing to the fluorescence emission. The color code used in c) and d) is the same, i.e. the fluorescence decay in blue corresponds to the species with the blue emission etc.

- ***Excitation at 780 nm***

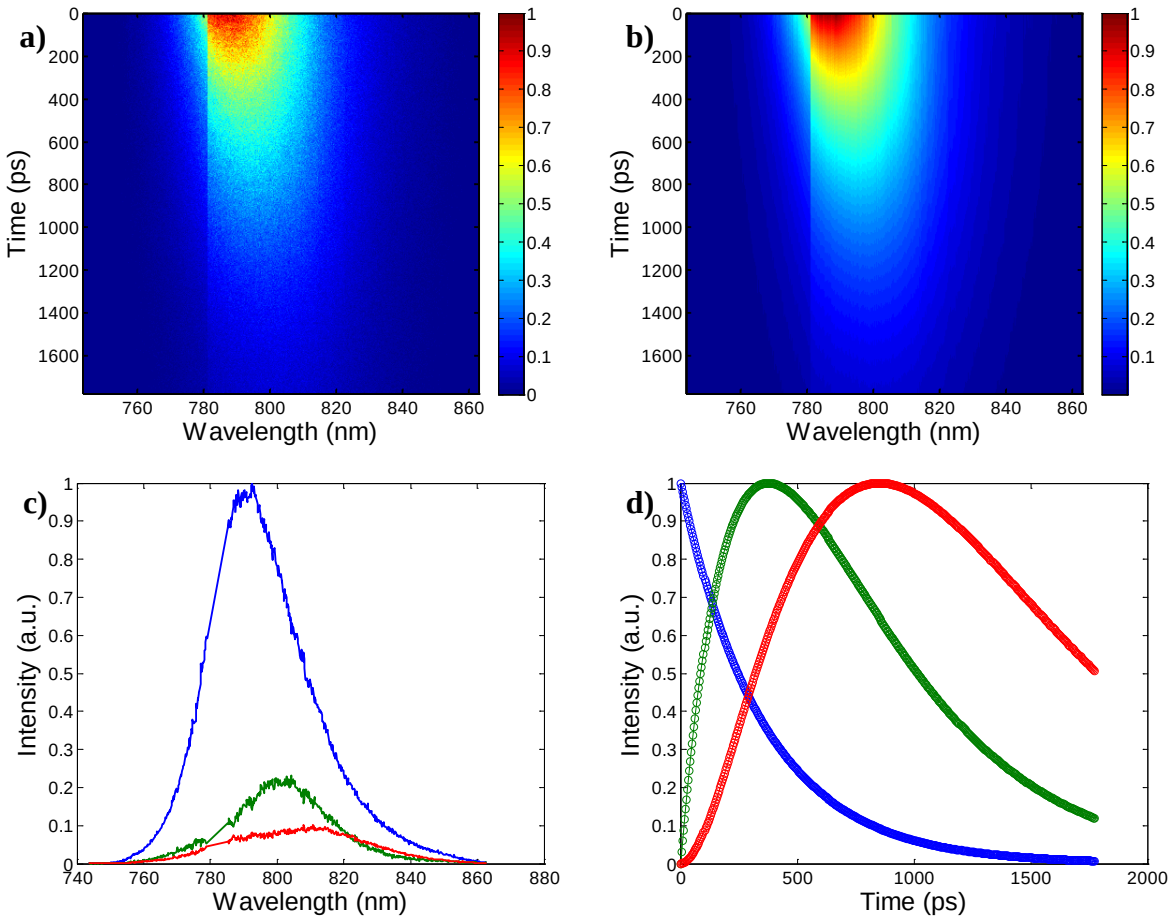

Figure S27. a) Normalized 2D streak camera image of the emission of $\mathbf{P_6}$ excited at 780 nm at 180 K in 2-MTHF with 1% pyridine. The image was corrected for the presence of excitation light scattering, and thus presents a gap of ca. 5 nm centered at λ_{exc}. b) Reconstructed 2D image of the emission of $\mathbf{P_6}$ excited at 840 nm. This image was built from data obtained in the fitting procedure. c) Spectral components and d) fluorescence decays of the 3 species contributing to the fluorescence emission. The color code used in c) and d) is the same, i.e. the fluorescence decay in blue corresponds to the species with the blue emission etc.

- ***Excitation at 820 nm***

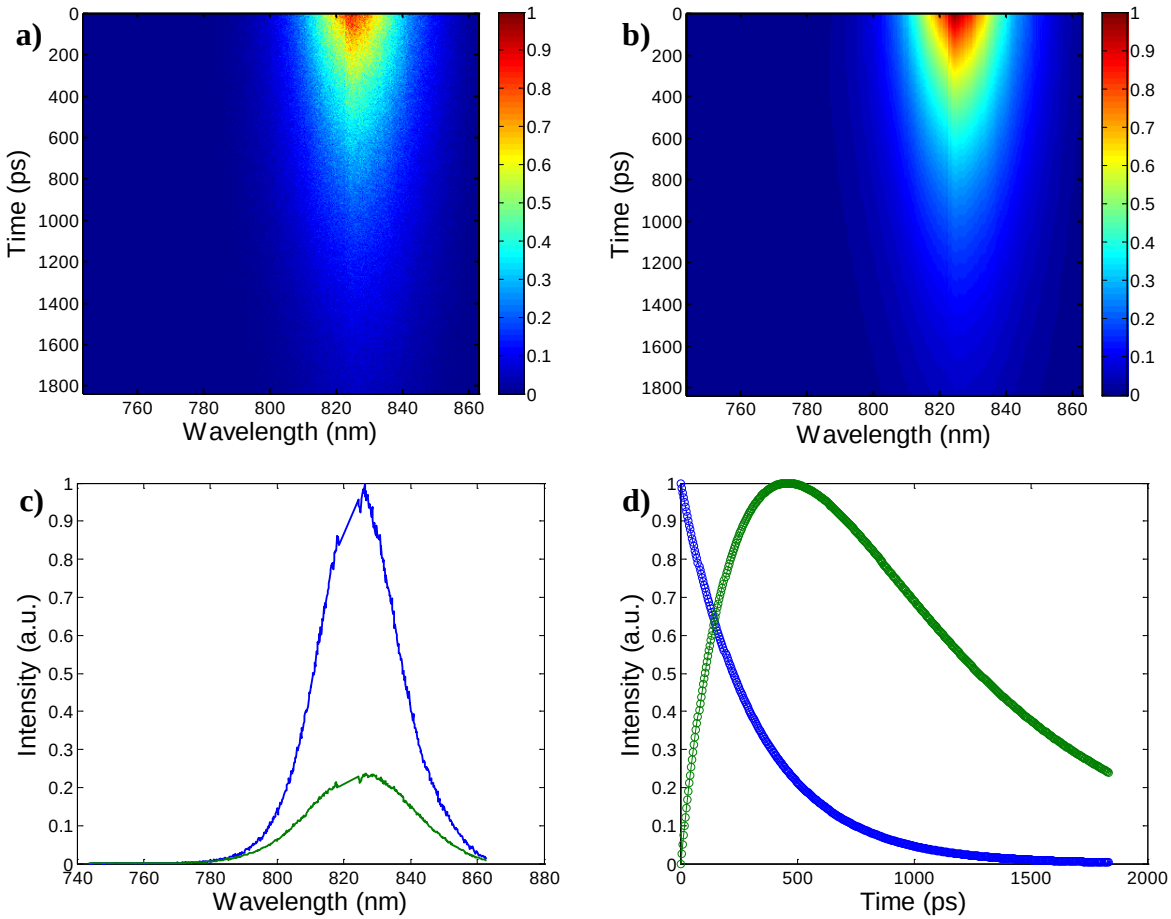

Figure S28. a) Normalized 2D streak camera image of the emission of $\mathbf{P_6}$ excited at 820 nm at 180 K in 2-MTHF with 1% pyridine. The image was corrected for the presence of excitation light scattering, and thus presents a gap of ca. 5 nm centered at λ_{exc}. b) Reconstructed 2D image of the emission of $\mathbf{P_6}$ excited at 840 nm. This image was built from data obtained in the fitting procedure. c) Spectral components and d) fluorescence decays of the 2 species contributing to the fluorescence emission. The color code used in c) and d) is the same, i.e. the fluorescence decay in blue corresponds to the species with the blue emission etc.

- ***Excitation at 840 nm***

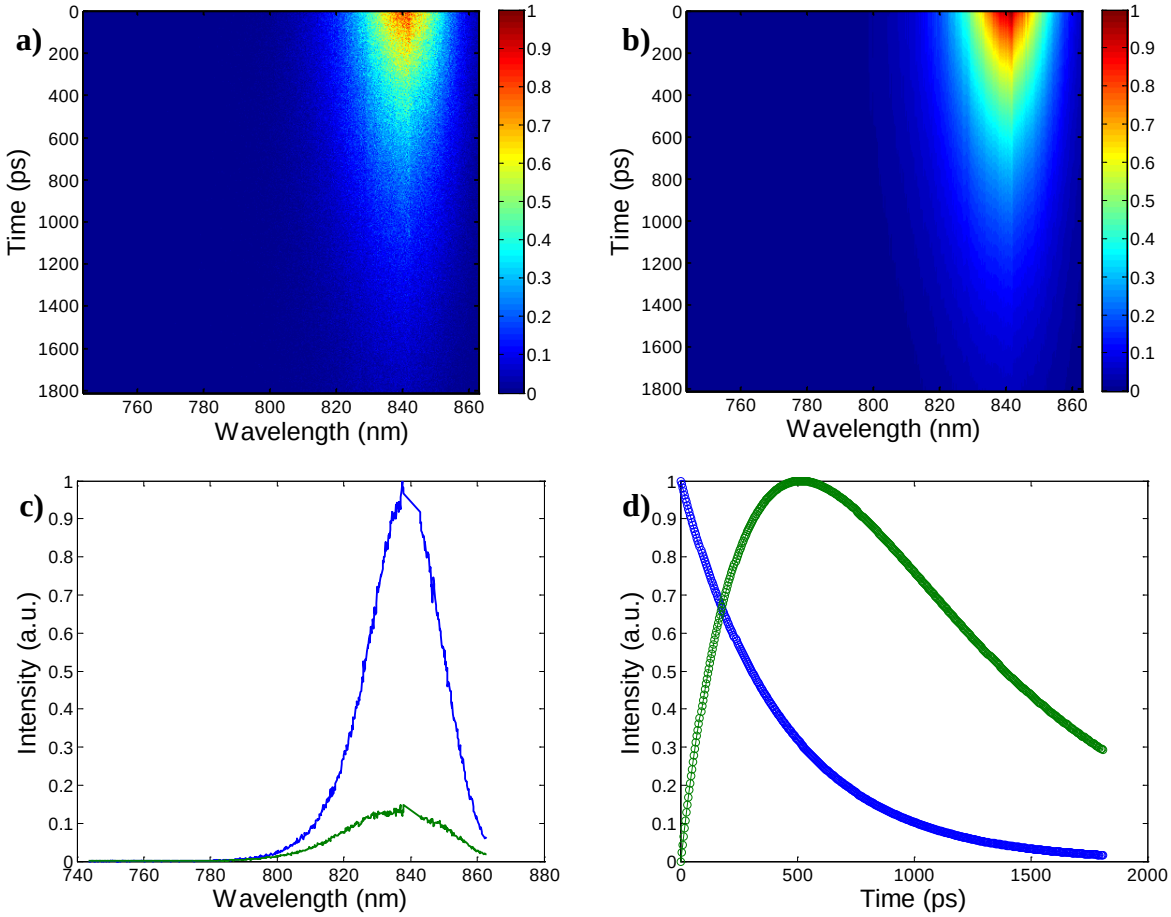

Figure S29. a) Normalized 2D streak camera image of the emission of $\mathbf{P_6}$ excited at 840 nm at 180 K in 2-MTHF with 1% pyridine. The image was corrected for the presence of excitation light scattering, and thus presents a gap of ca. 5 nm centered at λ_{exc}. b) Reconstructed 2D image of the emission of $\mathbf{P_6}$ excited at 840 nm. This image was built from data obtained in the fitting procedure. c) Spectral components and d) fluorescence decays of the 2 species contributing to the fluorescence emission. The color code used in c) and d) is the same, i.e. the fluorescence decay in blue corresponds to the species with the blue emission etc.

Analysis of 2D streak camera images of P_6C_{60} emission at 180 K

- ***Excitation at 730 nm***

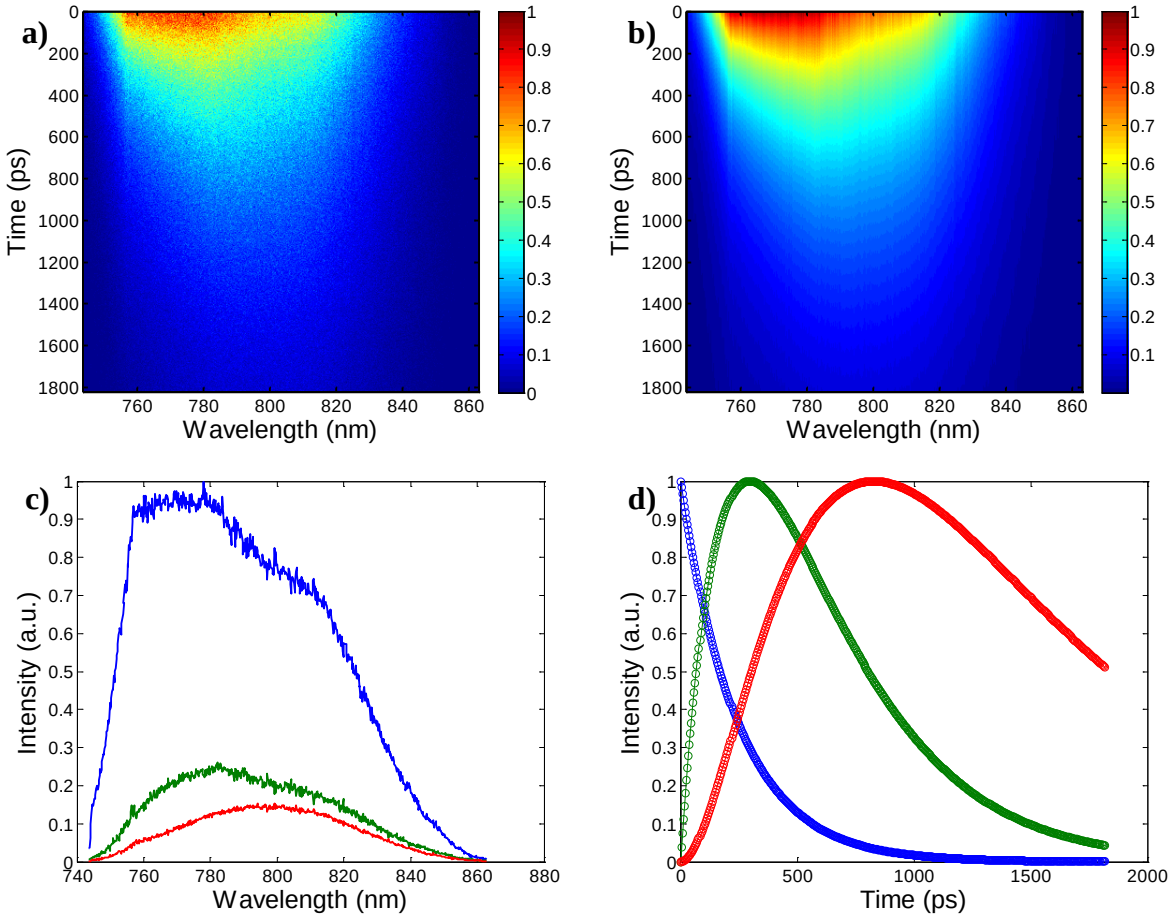

Figure S30. a) Normalized 2D streak camera image of the emission of $\mathbf{P_6}C_{60}$ excited at 730 nm at 180 K in 2-MTHF with 1% pyridine. b) Reconstructed 2D image of the emission of $\mathbf{P_6}C_{60}$ excited at 730 nm. This image was built from data obtained in the fitting procedure. c) Spectral components and d) fluorescence decays of the 3 species contributing to the fluorescence emission. The color code used in c) and d) is the same, i.e. the fluorescence decay in blue corresponds to the species with the blue emission etc.

- ***Excitation at 780 nm***

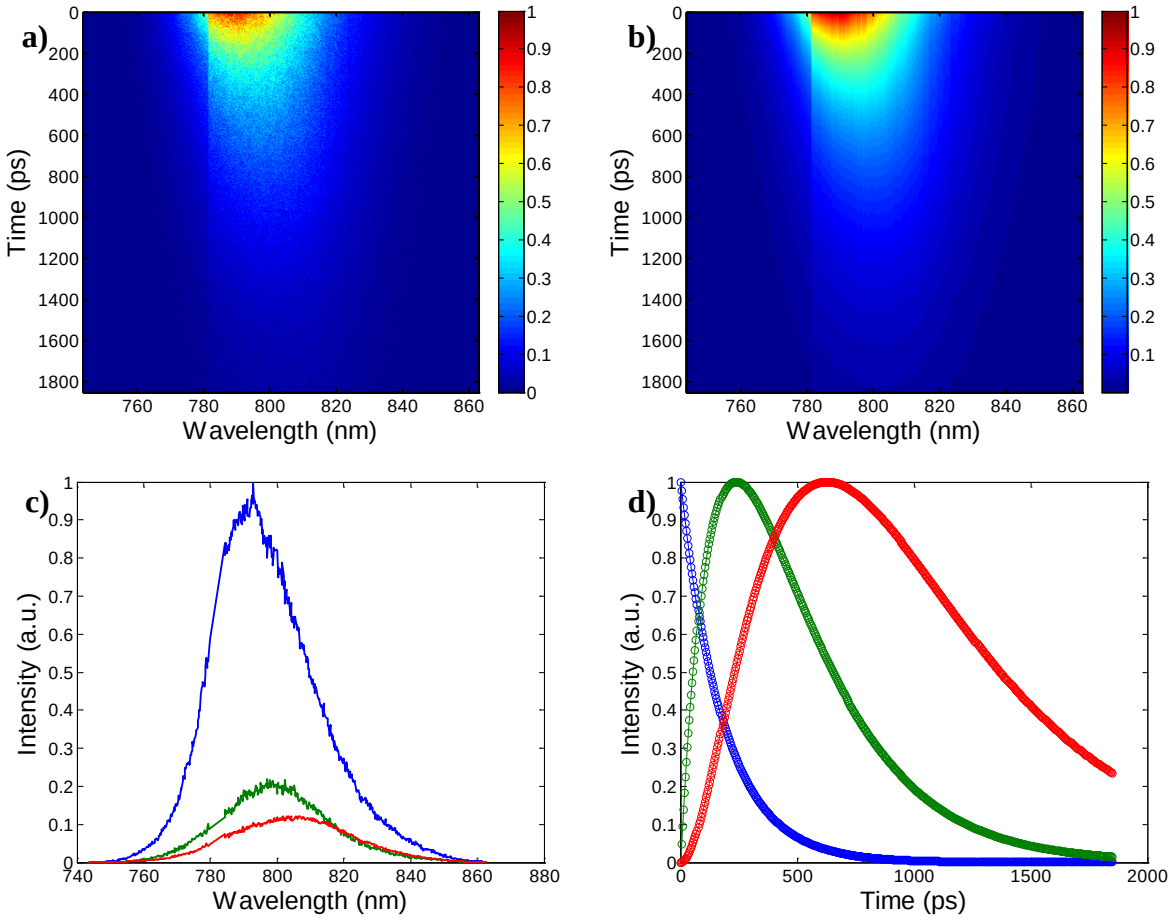

Figure S31. a) Normalized 2D streak camera image of the emission of $\mathbf{P_6C_{60}}$ excited at 780 nm at 180 K in 2-MTHF with 1% pyridine. The image was corrected for the presence of excitation light scattering, and thus presents a gap of ca. 5 nm centered at λ_{exc}. b) Reconstructed 2D image of the emission of $\mathbf{P_6C_{60}}$ excited at 780 nm. This image was built from data obtained in the fitting procedure. c) Spectral components and d) fluorescence decays of the 3 species contributing to the fluorescence emission. The color code used in c) and d) is the same, i.e. the fluorescence decay in blue corresponds to the species with the blue emission etc.

- ***Excitation at 820 nm***

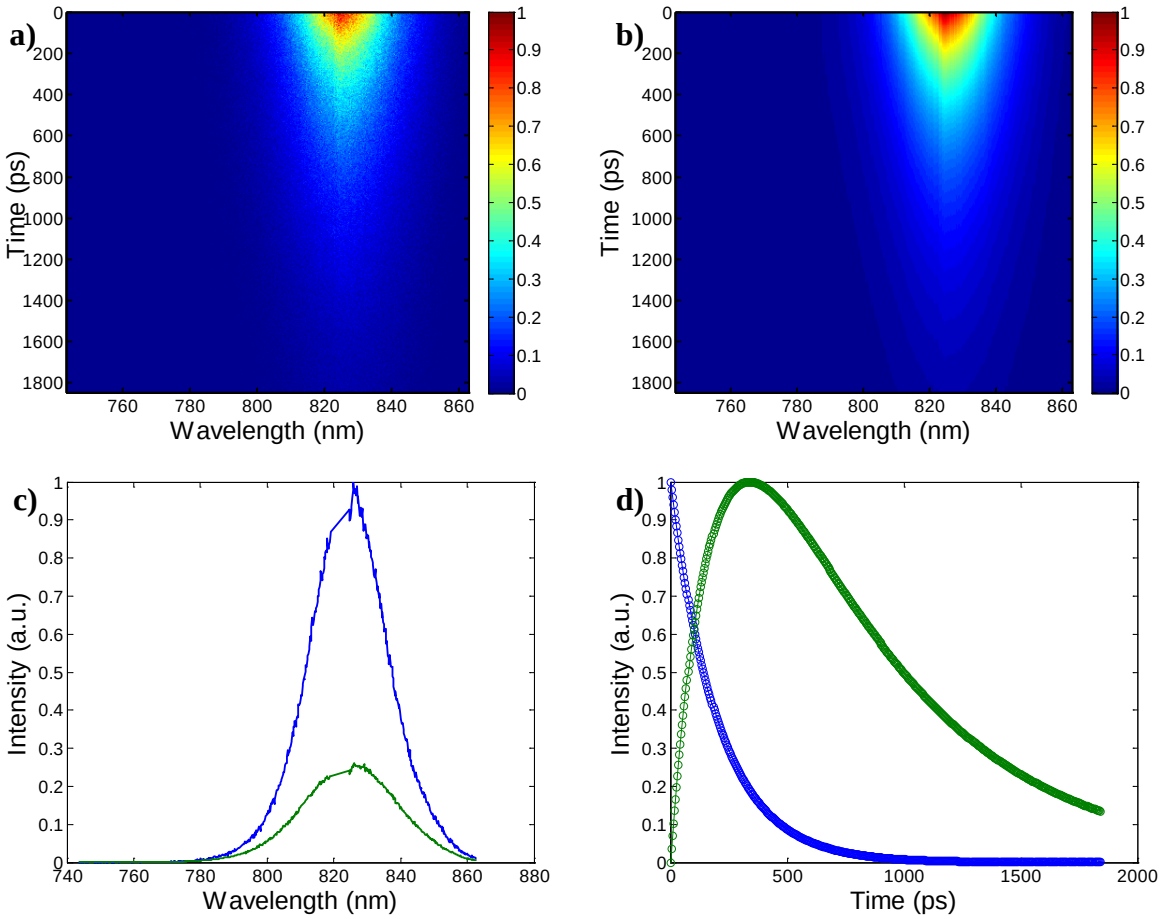

Figure S32. a) Normalized 2D streak camera image of the emission of $\mathbf{P_6}C_{60}$ excited at 820 nm at 180 K in 2-MTHF with 1% pyridine. The image was corrected for the presence of excitation light scattering, and thus presents a gap of ca. 5 nm centered at λ_{exc}. b) Reconstructed 2D image of the emission of $\mathbf{P_6}C_{60}$ excited at 820 nm. This image was built from data obtained in the fitting procedure. c) Spectral components and d) fluorescence decays of the 2 species contributing to the fluorescence emission. The color code used in c) and d) is the same, i.e. the fluorescence decay in blue corresponds to the species with the blue emission etc.

- ***Excitation at 840 nm***

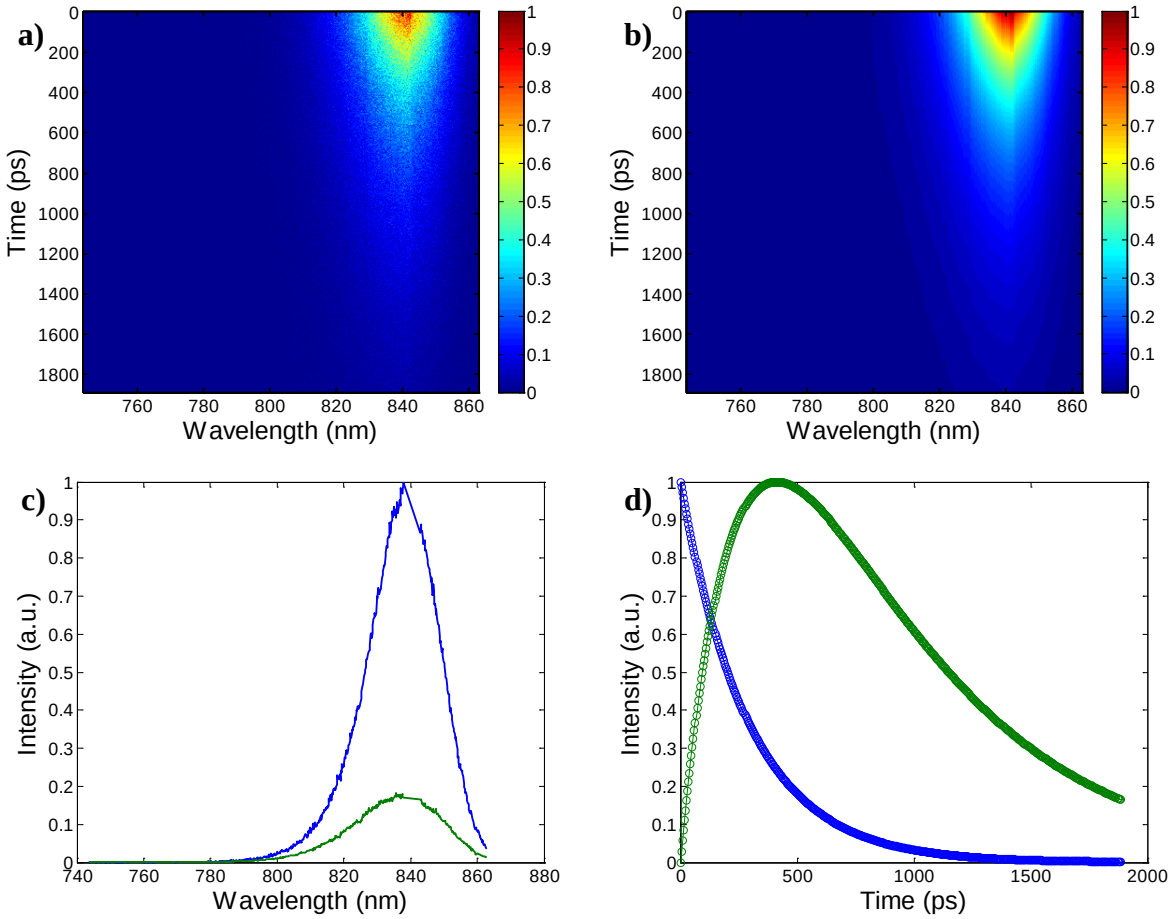

Figure S33. a) Normalized 2D streak camera image of the emission of $\mathbf{P_6}C_{60}$ excited at 840 nm at 180 K in 2-MTHF with 1% pyridine. The image was corrected for the presence of excitation light scattering, and thus presents a gap of ca. 5 nm centered at λ_{exc}. b) Reconstructed 2D image of the emission of $\mathbf{P_6}C_{60}$ excited at 840 nm. This image was built from data obtained in the fitting procedure. c) Spectral components and d) fluorescence decays of the 2 species contributing to the fluorescence emission. The color code used in c) and d) is the same, i.e. the fluorescence decay in blue corresponds to the species with the blue emission etc.

Fluorescence decays of P_6-T8 and P_6C_{60}-T8

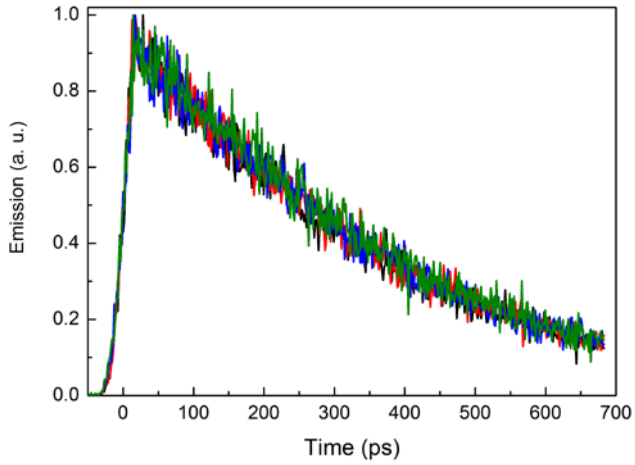

Figure S34. Extracted fluorescence decays of $\mathbf{P_6}C_{60}$-**T8** at 866 nm (black), 873 nm (red), 880 nm (blue) and 887 nm (green) using a streak camera. The excitation wavelength is 772 nm.

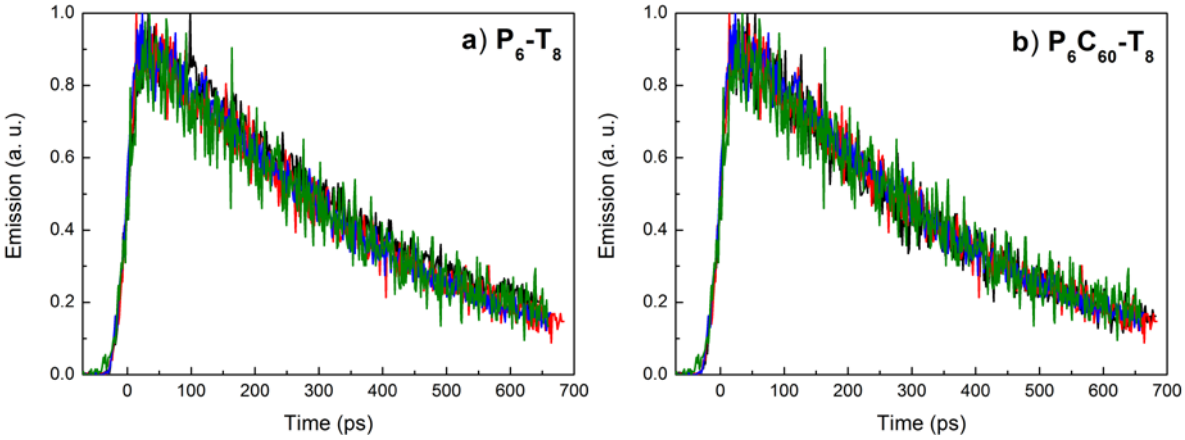

Figure S35. Extracted fluorescence decays of (a) $\mathbf{P_6}$-**T8** and (b) $\mathbf{P_6}C_{60}$-**T8** excited at 735 nm (black), 772 nm (red), 813 nm (blue) and 843 nm (green) using a streak camera. Emission wavelength was collected at 887 nm. The fluorescence decays could be globally fitted to a mono-exponential expression using an in-house built Matlab script.

Fluorescence decays of P_4-T8 and P_4C_{60}-T8

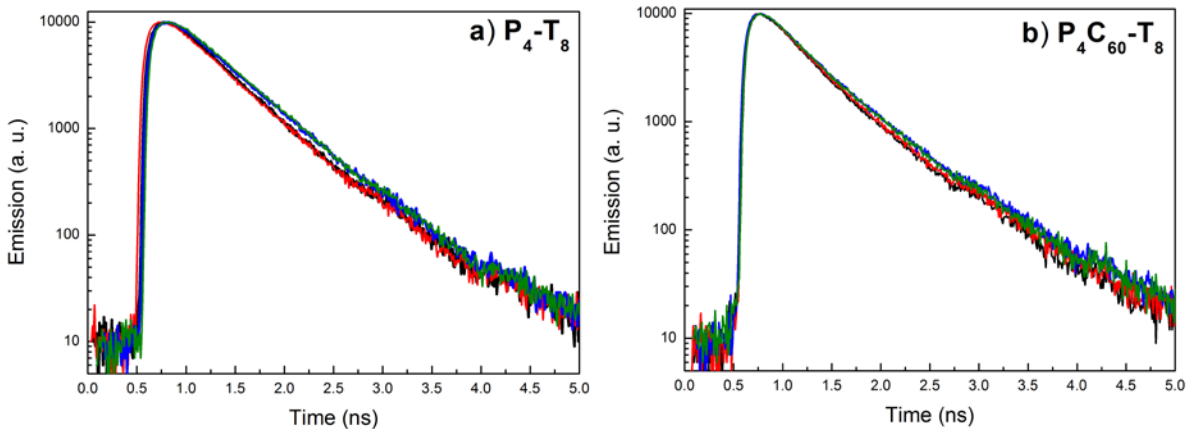

Figure S36. TCSPC measurements of (a) **P_4-T8** and (b) **P_4C_{60}-T8** excited at 735 nm (black), 765 nm (red), 820 nm (blue) and 840 nm (green). Emission was collected at 855 nm. All fluorescence decay curves were fitted to a mono-exponential expression using the program FluoFit Pro v.4 (PicoQuant GMBH) after deconvolution of the data with the IRF recorded for each excitation wavelength using a fused silica plate.

Table S6. Fluorescence lifetimes τ_f, rate constants for charge separation k_{CS} and quantum yield for charge separation ϕ_{CS} for P_nC_{60}-T8 complexes as function of the excitation wavelength

		Tetramer System		
λ_{exc} / nm	τ_f (**P_4-T8**) [a] / ps	τ_f (**P_4C_{60}-T8**) [a] / ps	k_{CS} [c] / s^{-1}	ϕ_{CS} [d]
735	499	398	5.1 x 10^8	0.20
765	499	405	4.7 x 10^8	0.19
820	527	414	5.2 x 10^8	0.21
840	530	417	5.1 x 10^8	0.21
		Hexamer System		
λ_{exc} / nm	τ_f (**P_6-T8**) [b] / ps	τ_f (**P_6C_{60}-T8**) [b] / ps	k_{CS} [c] / s^{-1}	ϕ_{CS} [d]
735	430	374	3.5 x 10^8	0.13
772	432	382	3.0 x 10^8	0.12
813	448	382	3.9 x 10^8	0.15
843	443	397	2.6 x 10^8	0.10

[a] The lifetimes were obtained from fitting the fluorescence decays measured using TCSPC. [b] The lifetimes were obtained from fitting the fluorescence decays measured using a streak camera system.

[c]The charge separation rate constant k_{CS} was determined using the formula $k_{CS}= 1/\tau_f$ (**P$_n$**C$_{60}$-**T8**) – $1/\tau_f$ (**P$_n$-T8**). [d] The quantum yield for charge separation ϕ_{CS} was calculated as $\phi_{CS}= k_{CS} \cdot \tau_f$ (**P$_n$**C$_{60}$-**T8**).

Determination of the excited states energies of P_nC_{60} systems

For the shorter oligomers $\mathbf{P_1}C_{60}$ and $\mathbf{P_2}C_{60}$, the calculated energies of the excited states correspond to the absorption maxima of the Q band that is attributed to the ($S_0 \rightarrow S_1$) transition.

In contrast for the longer oligomers $\mathbf{P_n}C_{60}$ (n = 3, 4, 6), a quantitative estimation of the position of the excited state energy levels is more difficult to obtain due to the broader distribution of conformers. Due to the broad and unstructured Q band of these oligomers, the upper energy level of the excited states is delicate to determine and is arbitrary estimated from the wavelength corresponding to the beginning of the Q band on the absorption spectra. Due to the uncertainty on the position of these upper energy levels, these levels are indicated as dashed lines on the energy diagram. The lower energy level of the excited states corresponds to the energy of the 0-0 transition, $E_{0\text{-}0.}$ This energy was obtained from the wavelength corresponding to the intersection of the normalized absorption and fluorescence spectra.

As for the charge-separated state $\mathbf{P_n}^{+}C_{60}^{-}$, the energy level was found to be independent of the oligomer size and was estimated from electrochemical data reported previously by Winters et al.[1]

References

(1) Winters, M. U.; Dahlstedt, E.; Blades, H. E.; Wilson, C. J.; Frampton, M. J.; Anderson, H. L.; Albinsson, B. *J. Am. Chem. Soc.* **2007**, *129*, 4291.